

Design and Synthesis of Potent Quinazolines as Selective β -Glucocerebrosidase Modulators

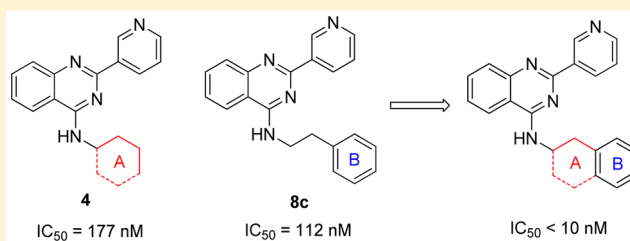
Jianbin Zheng,^{†,‡} Long Chen,[†] Michael Schwake,[†] Richard B. Silverman,^{*,‡} and Dimitri Krainc^{*,†}

[†]Department of Neurology, Northwestern University Feinberg School of Medicine, Chicago, Illinois 60611, United States

[‡]Department of Chemistry, Department of Molecular Biosciences, Chemistry of Life Processes Institute, Center for Molecular Innovation and Drug Discovery, and Center for Developmental Therapeutics, Northwestern University, Evanston, Illinois 60208-3113, United States

S Supporting Information

ABSTRACT: Gaucher's disease is a common genetic disease caused by mutations in the β -glucocerebrosidase (GBA1) gene that have been also linked to increased risk of Parkinson's disease and Lewy body dementia. Stabilization of misfolded mutant β -glucocerebrosidase (GCase) represents an important therapeutic strategy in synucleinopathies. Here we report a novel class of GCase quinazoline inhibitors, obtained in a high throughput screening, with moderate potency against wild-type GCase. Rational design and a SAR study of this class of compounds led to a new series of quinazoline derivatives with single-digit nanomolar potency. These compounds were shown to selectively stabilize GCase when compared to other lysosomal enzymes and to increase N370S mutant GCase protein concentration and activity in cell assays. To the best of our knowledge, these molecules are the most potent noniminosugar GCase modulators to date that may prove useful for future mechanistic studies and therapeutic approaches in Gaucher's and Parkinson's diseases.



■ INTRODUCTION

Gaucher's disease (GD), the most common lysosomal storage disease, is caused by a recessively inherited deficiency in β -glucocerebrosidase (GCase) and subsequent accumulation of glucoceramides, toxic lipid substrates.^{1,2} Substrate accumulation leads to hepatosplenomegaly, bone marrow suppression, and bone lesions.^{1–3} Many of the GCase mutations are missense mutations⁴ that result in single amino acid substitutions of the enzyme. Most of these mutations, including the prevalent N370S mutation, are still functional, although with very low residual GCase activity⁵ due to enzyme misfolding and proteasome-mediated breakdown.⁵ Current treatments for GD include enzyme replacement therapy (ERT) and substrate reduction therapy (SRT).^{2,6} In recent years, mutations in GBA1 were also found to be a major risk factor for Parkinson's disease (PD) and dementia with Lewy bodies (DLB).^{7–11} Accumulation of β -glucosylceramide, the substrate of GCase, in neurons promotes the formation of α -synuclein oligomers, which are considered toxic in PD.¹² Enhancement of GCase activity is thought to be a potential therapeutic strategy for GCase-associated synucleinopathies, including PD.^{13,14}

An emerging therapeutic approach involves the restoration of proper folding and lysosome delivery of degradation-prone mutant enzymes using small molecules as pharmacological chaperones (PCs).⁵ Previous studies have shown that iminosugars increase the cellular activity of the N370S mutant form of GCase,^{15,16} as well as of the wild-type enzyme.^{5,17} Isfagomine (IFG, 1) attracted the most attention in the

iminosugar class of compounds (Figure 1).¹⁸ However, iminosugars tend to have poor selectivity and relatively short half-lives in cells.¹⁹ Several different scaffolds of noniminosugar inhibitors (2 and 3 are examples in Figure 1) have been

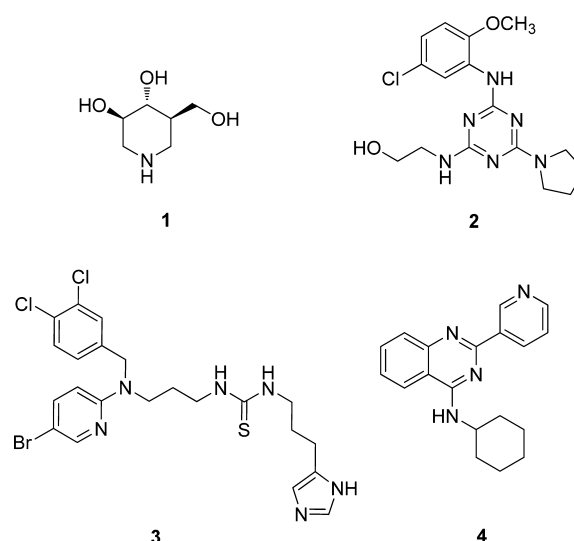
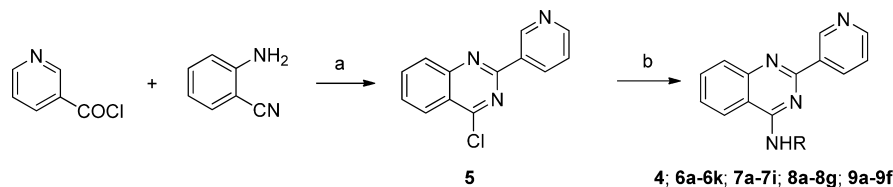


Figure 1. Structures of GCase inhibitors.

Received: June 22, 2016

Scheme 1. Synthesis of 4, 6a–6k, 7a–7i, 8a–8g, and 9a–9f with Substituents on the Secondary Amine^a

^aReagents and conditions: (a) (i) sulfolane, (ii) PCl_5 ; (b) RNH_2 , K_2CO_3 , DMF

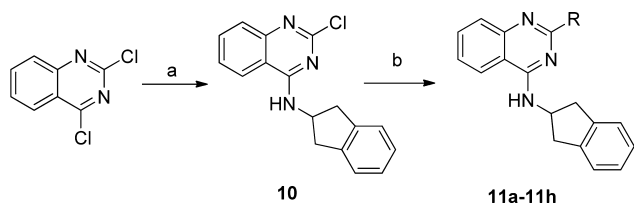
reported as GCCase PCs since 2007;^{20–24} however, the binding site and the interaction with GCCase of these noniminosugar PCs remain unknown.

In our high throughput screening effort to discover potent GCCase modulators, compound 4 (Figure 1) was identified as a potent GCCase inhibitor (IC_{50} 0.177 μM) in a 4-methylumbelliferyl β -D-glucopyranoside (4MU- β -Glc) enzyme activity based high throughput screen. The activity was confirmed with additional synthesized compounds. To further develop potent GCCase modulators and use them to explore the properties of the binding site, we carried out a structure–activity relationship (SAR) study of a series of quinazoline derivatives, leading to the discovery of single-digit nanomolar potency GCCase inhibitory modulators.

CHEMISTRY

The synthesis of compound 4 and its analogues for SAR exploration is straightforward and is detailed in Schemes 1 and 2. As showed in Scheme 1, 5 was prepared from 2-aminobenzonitrile and nicotinoyl chloride according to a known method.²⁵ The reaction of 5 and appropriate amines in the presence of potassium carbonate as a base afforded 4, 6a–6k, 7a–7i, 8a–8g, and 9a–9f.

Additional analogues having modifications at position 2 of the quinazoline ring were synthesized, employing alkylation of 2,3-dihydro-1H-inden-2-amine with 2,4-dichloroquinazoline, followed by Suzuki coupling with appropriate boronic acids to afford 11a–11h (Scheme 2). The structure and purity of all the prepared compounds were confirmed by spectroscopic and analytical techniques.

Scheme 2. Synthesis of 11a–11h with Modifications at the 2-Position of the Quinazoline Ring^a

^aReagents and conditions: (a) 2,3-dihydro-1H-inden-2-amine, K_2CO_3 , DMF; (b) RB(OH)_2 , $\text{Pd(PPh}_3)_4$, K_2CO_3 , 1,4-dioxane, H_2O

RESULTS AND DISCUSSION

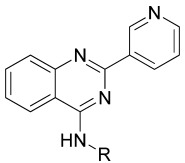
In our high throughput screening efforts to discover potent GCCase inhibitors/activators, we used recombinant wild-type GCCase and 4MU- β -Glc as substrate in an optimized pH 5.9 buffer.²⁶ In previous studies, high concentrations of taurocholate (4–10 mM) were used to improve the signal in GCCase enzyme activity assays.^{16,27,28} We found that taurocholate can

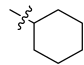
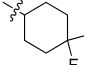
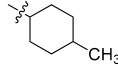
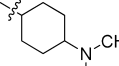
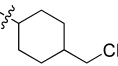
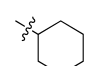
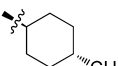
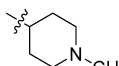
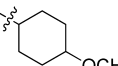
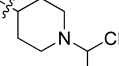
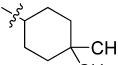
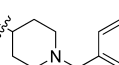
interfere with our assay results, which was also reported recently by Berger et al.;²⁹ therefore, we excluded taurocholate in our screening assay. Using this approach, we discovered several different scaffolds of GCCase inhibitors and activators with moderate activity. Among these, we identified a quinazoline compound (4, Figure 1) as a potent GCCase inhibitor. The quinazoline ring had previously been found as the best scaffold for GCCase inhibitors among several ring systems assayed.²¹ Here we describe our modifications of the substituents on the quinazoline ring.

To examine the SAR at the amino group, a series of substituents was introduced at the 4-position of the *N*-cyclohexyl ring of 4 (Table 1). A 4-methyl substituent (6a, *cis/trans* = 3/2 mixture) resulted in 3-fold higher activity (IC_{50} 56 nM), while 4-ethyl substitution (6b, *cis/trans* = 3/2 mixture) did not show a significant change of activity, suggesting that a smaller hydrophobic group at this position may be beneficial. Then, a *trans*-4-methyl compound (6c) was synthesized, which exhibited great improvement of inhibitory activity (IC_{50} 20 nM). Further modification by installation of 4-methoxyl (6d), 4,4-dimethyl (6e), or 4,4-difluoro (6f) groups at the same position decreased the potency; dimethylaminocyclohexyl (6g) and *N*-methylpiperidino (6i) substituents were detrimental to activity. Replacement of the cyclohexyl group by tetrahydro-2H-pyran-3-yl (6h) or *N*-substituted piperidine (6i–6k) afforded weak or inactive compounds, supporting the importance of the lipophilic cyclohexyl ring.

To further expand the SAR of the amino group, the cyclohexyl ring of 4 was replaced by a series of saturated carbon rings of different sizes. A dramatic SAR was observed with different carbon rings (7a–7e). As shown in Table 2, the larger cycloalkyl rings were more potent; the compound with a cyclooctyl group (7a, IC_{50} 27 nM) was the most potent. However, when bulk was introduced to the cycloalkyl ring, the potency of the compounds (7f and 7g) decreased, suggesting that the hydrophobic binding pocket may be compact. Introduction of one or two carbons between the cyclohexyl and NH groups (7h and 7i) in 4 decreased the inhibitory activity, again indicating a hydrophobic pocket with limited volume.

To understand the nature of the binding site, a phenyl ring with different length linkers was introduced into the molecules (8a–8e, Table 3). Compound 8a, by replacement of the cyclohexyl ring in 4 with a phenyl ring, lost activity. Insertion of a 1–4 carbon linker between the phenyl and quinazoline rings gave 8b–8e. Interestingly, 8c, with a phenylethyl group, was slightly more potent than 4. Extension of the linker did not benefit activity, suggesting that a two carbon length linker between the phenyl ring and secondary amino group of 8c may allow optimal binding of the phenyl group. Substitution of the phenyl group in 8 with a 2- or 3-pyridine ring (8f or 8g) sharply

Table 1. Structure and Inhibitory Activity of 2-(Pyridin-3-yl)quinazoline Derivatives with Substituted Cyclohexyl and Related Rings^a


Comp.	R	IC ₅₀ (μM)	Comp.	R	IC ₅₀ (μM)
4		0.177 ± 0.012	6f		0.234 ± 0.017
6a	 (Cis/Trans: 3/2)	0.056 ± 0.005	6g		Inactive
6b	 (Cis/Trans: 3/2)	0.126 ± 0.007	6h		0.891 ± 0.023
6c		0.020 ± 0.002	6i		Inactive
6d		0.251 ± 0.018	6j		33.21 ± 9.71
6e		0.431 ± 0.042	6k		36.07 ± 8.72

^aExperiments were performed in triplicate, and the mean ± SD is shown.

diminished potency, indicating a repulsive effect of the pyridine nitrogen atom.

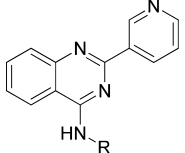
To enhance the binding affinity of the compounds with GCCase, a new series of compounds was designed to integrate both the hydrophobic interaction of the A ring and the π - π interaction of the B ring by fusing the cyclohexyl ring (**4**) with a phenyl ring (Figure 2 and Table 4). These derivatives (**9a**–**9c**) exhibited single-digit nanomolar inhibitory activity against GCCase. Stereochemistry did not seem to be important (**9a** and **9b**). The compound with an indane ring (**9c**) gave comparable activity to that of the tetralin ring (**9a**). Attachment of the quinazoline ring to the tetralin ring (**9d**) and indane ring (**9e**) at position 1 instead of position 2 (**9a** and **9c**) dramatically increased the IC₅₀ values to the low micromolar range, indicating the importance of the orientation of this substituent for binding activity of these inhibitors. The introduction of an oxygen atom to give a chromane (**9f**) did not significantly affect the potency. These results suggest important hydrophobic and π - π interactions in the binding of this series of compounds to GCCase.

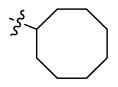

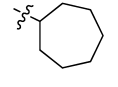
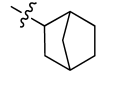
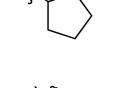
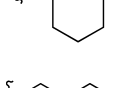
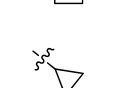
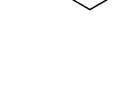
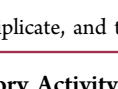
Finally, we examined the substituent effect on the pyridine ring. A methyl group was introduced at different positions of the 3-pyridinyl ring of **9c** to give **11a**–**11c** (Table 5). Methylation of the pyridine ring decreased the potency. Whereas the compound with a methyl group at position 4 of the pyridinyl ring (**11a**) showed only moderate potency, the

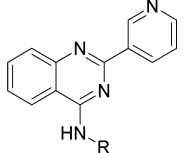
other two compounds (**11b** and **11c**) with a methyl group at positions 5 and 6 were much more potent, comparable to that when a 2-furanyl group replaced the pyridine ring but still not as potent as **9c**. The replacement of the 3-pyridinyl ring in **9c** with either phenyl (**11d**) or 3-thienyl (**11g**) groups, however, gave compounds that retained the same potency as **9c**, suggesting that more groups could be introduced at position 2 of the quinazoline ring.

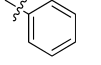
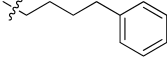
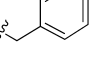
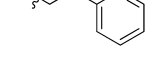
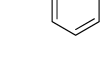
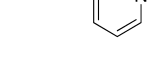
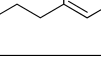
We also evaluated the activity of these selected compounds at various pH values (Table 6). Interestingly, compared to the inhibitory activity at pH 5.9, the activity of **9a**, **9b**, and **9c** with a 3-pyridinyl ring decreased by 3-fold at pH 5.0, while the activity of **11d**, **11f**, and **11g** only dropped slightly at both pH conditions. Although the cause for the change in IC₅₀ values is not clear, an explanation may involve the protonation state of the compounds or the variability of the enzyme efficacy at different pH values.

Compounds shown to act as pharmacological chaperones for GCCase (or other lysosomal enzymes) also stabilize the enzyme against thermal denaturation. A fluorescent thermal shift assay was developed to evaluate the binding affinity of ligands with protein.³⁰ To evaluate their abilities to stabilize GCCase, the most potent compounds, **9a**, **9b**, **11d**, **11f**, and **11g**, were accessed in a wild-type GCCase fluorescent thermal shift assay with a negative control (**8a**) and a positive control (IFG) at pH 5.0. The selected compounds increased the GCCase melting

Table 2. Structure and Inhibitory Activity of 2-(Pyridin-3-yl)quinazoline Derivatives with Saturated Alkyl Rings^a


Comp.	R	IC ₅₀ (μM)	Comp.	R	IC ₅₀ (μM)
7a		0.027 ± 0.002	7f		0.926 ± 0.08
7b		0.042 ± 0.003	7g		0.282 ± 0.043
7c		0.72 ± 0.05	7h		0.405 ± 0.040
7d		2.84 ± 0.34	7i		0.857 ± 0.033
7e		28.07 ± 3.21			

^aExperiments were performed in triplicate, and the mean ± SD is shown.Table 3. Structure and Inhibitory Activity of 2-(Pyridin-3-yl)quinazoline Derivatives with Aromatic Rings^a


Comp.	R	IC ₅₀ (μM)	Comp.	R	IC ₅₀ (μM)
8a		inactive	8e		1.28 ± 0.13
8b		5.77 ± 0.82	8f		1.40 ± 0.12
8c		0.097 ± 0.009	8g		4.29 ± 0.57
8d		1.53 ± 0.22			

^aExperiments were performed in triplicate, and the mean ± SD is shown.

point in a dose-dependent manner (Figure 3), while inactive compound 8a did not change the melting points significantly. Most compounds exhibited greater ability to stabilize GCase than IFG at lower concentrations, and 11g showed the maximum thermal shift up to around 11 °C. It should be noted that the increment in melting point has a direct correlation with the compound's binding affinity.³¹ The maximum thermal shift of our compounds corresponded to

their inhibitory activity at pH 5.0, suggesting a close correlation of the binding affinity and the inhibitory activity for these compounds.

The selected compounds (9a, 9b, 11d, 11g, and 11f) were further evaluated against two other lysosomal hydrolases, acid α-glucosidase (GAA) and α-galactosidase A (GLA). The activities of tested enzymes were not significantly changed by

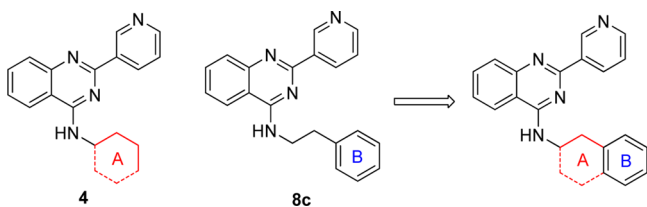


Figure 2. Rational design of a new series of potent quinazoline inhibitors.

compound treatments up to 100 μM (representative results shown for **11g** in Figure 4).

We further tested compounds **4** and **11g** by measuring GCase activity at various substrate concentrations (30–150 μM) and in the absence or presence of increasing concentrations of GCase inhibitors. Similarly to reported noniminosugar inhibitors,²⁰ both of our inhibitors exhibited linear mixed inhibition, with an increase in K_m and decrease in V_{max} values upon increasing inhibitor concentrations (Figure 5A,B).

Finally, we tested **11g** in patient-derived N370S fibroblasts. The fibroblasts were treated with **11g** and IFG for 3 days, and levels of GCase protein were determined by immunoblot. We found that **11g** treatments (2, 5, and 10 μM) increased the level of GCase, while IFG showed a similar effect only at the higher concentrations (20 and 50 μM) (Figure 6, top). We also used endoH and PNGase F to digest the cell lysates to determine whether **11g** treatment affected GCase maturation. The immunoblot (Figure 6, middle) showed that most of the GCase bands were resistant to endoH digestion, indicating that the major GCase signal after treatment is a post-ER form. PNGase F digestion gave a single band with increased GCase concentration after **11g** treatment (Figure 6, bottom). In addition to this finding, we also found that a 3-day treatment of compound **11g** (2 μM) increased 50% of GCase activity in a separate enzyme activity assay, suggesting that **11g** increased both GCase levels and the activity of patient-derived N370S fibroblasts.

CONCLUSIONS

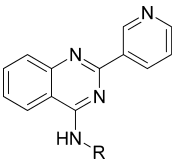
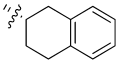
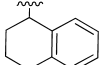
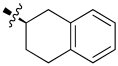
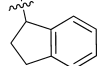
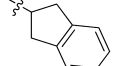
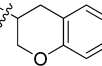
In this paper, we describe the design and SAR of a series of quinazoline GCase inhibitors having single-digit nanomolar potency. The SAR suggested that a hydrophobic interaction and a π – π interaction may be involved in compound binding to GCase. These quinazoline derivatives also stabilized GCase, as indicated by thermal shift assays, and exhibited high selectivity against other lysosomal hydrolases. Furthermore, the most potent compound (**11g**) increased the mature post-ER form of GCase and the enzyme activity in patient-derived N370S fibroblasts. It will be of interest to further test these compounds in other biological assays and models of Gaucher's and Parkinson's disease.

EXPERIMENTAL SECTION

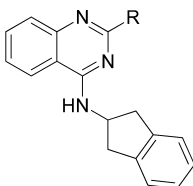
Materials and Methods. Chemistry. Commercially available reagents and solvents were used without further purification. All reactions were monitored by thin-layer chromatography (TLC) using 0.25 mm Silicycle extra hard 250 μM TLC plates (60 F254). Purification of reaction products was carried out by flash chromatography using an Agilent 971-FP flash purification system with Silicycle silica gel columns. The yields are not optimized. The purity of all compounds was over 95% as analyzed with an Agilent 1260 Infinity HPLC system and an Agilent Poroshell 120 EC-C18 (4.6 mm \times 50 mm, 2.7 μm) reverse phase column, detecting with UV absorbance (254 nm). ^1H NMR and ^{13}C NMR spectra were obtained using a Bruker Avance III 500 MHz system (500 MHz for ^1H NMR and 125 MHz for ^{13}C NMR) spectrometer. Chemical shifts are reported relative to chloroform ($\delta = 7.26$ for ^1H NMR and $\delta = 77.16$ for ^{13}C NMR spectra) or dimethyl sulfoxide ($\delta = 2.50$ for ^1H and $\delta = 39.52$ for ^{13}C NMR spectra). Data are reported as br = broad, s = singlet, d = doublet, t = triplet, q = quartet, m = multiplet. Mass spectra were obtained using a Bruker AmaZon SL system. High resolution mass spectra (HRMS) were performed using an Agilent 6210A LC-TOF instrument with a dual spray ESI source, with a high resolution time-of-flight (TOF) mass analyzer and collecting in a 2 GHz detector mode coupled with an Agilent 1200 HPLC.

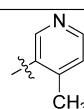
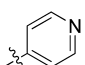
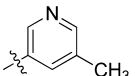
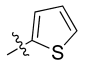
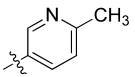
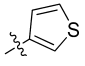
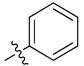
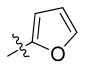
Preparation of 4-Chloro-2-(pyridin-3-yl)quinazoline (5).²⁵ To a solution of 2-aminobenzonitrile (5.90 g, 50 mmol) in sulfolane (20 mL) was added nicotinoyl chloride hydrochloride (12.0 g, 67.4 mmol), and the mixture was stirred at 100 $^\circ\text{C}$ for 16 h. PCl_5 (18.2 g, 87.5

Table 4. Structure and Inhibitory Activity of 2-(Pyridin-3-yl)quinazoline Derivatives with Fused Rings^a

					
Comp.	R	IC ₅₀ (nM)	Comp.	R	IC ₅₀ (nM)
9a		8.7 \pm 1.1	9d		872 \pm 71
9b		9.9 \pm 1.3	9e		821 \pm 73
9c		8.3 \pm 1.0	9f		35 \pm 3

^aExperiments were performed in triplicate, and the mean \pm SD is shown.

Table 5. Structure and Inhibitory Activity of 4-(2,3-Dihydro-1H-2-indenamino)quinazoline Derivatives with Aromatic Rings^a


Comp.	R	IC ₅₀ (nM)	Comp.	R	IC ₅₀ (nM)
11a		122 ± 12	11e		168 ± 18
11b		12.5 ± 1.7	11f		8.2 ± 1.0
11c		29.4 ± 3.6	11g		5.2 ± 0.6
11d		6.5 ± 0.7	11h		21.1 ± 2.4

^aExperiments were performed in triplicate, and the mean ± SD is shown.

mmol) was added in one portion and stirred at 100 °C for 10 h. The mixture was cooled to room temperature and carefully poured into 400 mL of saturated sodium bicarbonate solution cooling in an ice bath. The solid was filtered, washed with water, dried, and purified by flash chromatography to give **5** as a pale-yellow solid (5.50 g, 46%); mp 160–163 °C. ¹H NMR (400 MHz, CDCl₃) δ 9.76 (d, *J* = 1.3 Hz, 1H), 8.82 (dt, *J* = 8.0, 1.9 Hz, 1H), 8.73 (dd, *J* = 4.7, 1.4 Hz, 1H), 8.26 (dd, *J* = 8.4, 0.8 Hz, 1H), 8.10 (d, *J* = 8.4 Hz, 1H), 7.95 (ddd, *J* = 8.4, 7.0, 1.4 Hz, 1H), 7.69 (ddd, *J* = 8.2, 7.0, 1.1 Hz, 1H), 7.44 (dd, *J* = 7.5, 4.8 Hz, 1H). ¹³C NMR (100 MHz, CDCl₃) δ 162.9, 158.3, 151.8, 151.7, 150.3, 136.1, 135.2, 132.4, 129.1, 128.9, 126.0, 123.5, 122.8. ESI-MS *m/z*: 242 (*M* + H)⁺.

General Procedure for Compounds 4, 6a–6k, 7a–7i, 8a–8g, and 9a–9f. A mixture of 4-chloro-2-(pyridin-3-yl)quinazoline **5** (72 mg, 0.3 mmol), amine (0.3 mmol), and potassium carbonate (69 mg, 0.3 mmol) in DMF (3 mL) was stirred at room temperature or 60 °C overnight. Water (20 mL) was added, and the formed solid was filtered, washed with water, and dried in vacuo to give product. The products were usually pure (>95% purity). Those products without sufficient purity were purified by flash chromatography.

Analytical Data for Compounds. *N*-Cyclohexyl-2-(pyridin-3-yl)quinazolin-4-amine (**4**). Off-white solid (64 mg, 70%); mp 108–111 °C. ¹H NMR (500 MHz, CDCl₃) δ 9.74 (s, 1H), 8.84 (d, *J* = 6.6 Hz, 1H), 8.70 (s, 1H), 7.95 (d, *J* = 7.1 Hz, 1H), 7.74 (t, *J* = 7.7 Hz, 2H), 7.49–7.35 (m, 2H), 5.77 (s, 1H), 4.48–4.32 (m, 1H), 2.28–2.20 (m, 2H), 1.93–1.79 (m, 2H), 1.79–1.67 (m, 1H), 1.61–1.46 (m, 2H), 1.46–1.23 (m, 3H). ¹³C NMR (125 MHz, CDCl₃) δ 158.9, 158.8, 150.7, 150.5, 150.3, 135.7, 134.6, 132.7, 129.0, 125.8, 123.2, 120.5, 113.9, 50.1, 33.0, 25.9, 25.1. HRMS (ESI): calcd for C₁₉H₂₁N₄ [*M* + H]⁺, 305.1761; found, 305.1764.

N-(4-Methylcyclohexyl)-2-(pyridin-3-yl)quinazolin-4-amine (*cis/trans* = 3/2) (**6a**). White solid (54 mg, 43%); mp 130–134 °C. *Cis* isomer: ¹H NMR (500 MHz, CDCl₃) δ 9.75 (s, 1H), 8.80 (d, *J* = 7.8 Hz, 1H), 8.69 (s, 1H), 7.92 (d, *J* = 8.3 Hz, 1H), 7.77–7.71 (m, 2H), 7.48–7.39 (m, 2H), 5.87 (d, *J* = 5.8 Hz, 1H), 4.65–4.58 (m, 1H), 2.02–1.94 (m, 2H), 1.86–1.81 (m, 2H), 1.76–1.62 (m, 3H), 1.36–1.21 (m, 2H), 1.00 (d, *J* = 6.5 Hz, 3H). ¹³C NMR (125 MHz, CDCl₃) δ 159.0, 158.8, 150.8, 150.4, 150.3, 135.8, 134.5, 132.8, 128.8, 125.9, 123.3, 120.5, 113.9, 47.2, 30.8, 30.4, 29.2, 21.3. *Trans* isomer: ¹H NMR

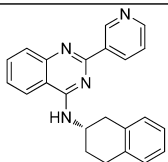
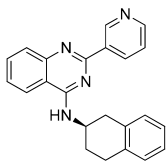
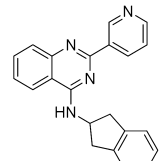
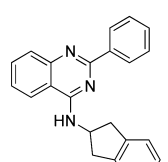
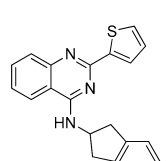
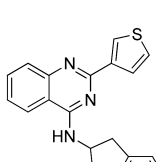
(500 MHz, CDCl₃) δ 9.75 (s, 1H), 8.80 (d, *J* = 7.8 Hz, 1H), 8.69 (s, 1H), 7.92 (d, *J* = 8.3 Hz, 1H), 7.77–7.70 (m, 2H), 7.48–7.39 (m, 2H), 5.63 (d, *J* = 5.3 Hz, 1H), 4.38–4.26 (m, 1H), 2.28 (d, *J* = 9.9 Hz, 2H), 1.86–1.81 (m, 2H), 1.54–1.40 (m, 1H), 1.40–1.30 (m, 2H), 1.30–1.14 (m, 2H), 0.98 (d, *J* = 6.5 Hz, 3H). ¹³C NMR (125 MHz, CDCl₃) δ 159.1, 158.8, 150.8, 150.5, 150.4, 135.8, 134.5, 132.8, 129.0, 125.9, 123.3, 120.7, 114.0, 50.5, 34.1, 33.1, 32.3, 22.4. HRMS (ESI): calcd for C₂₀H₂₃N₄ [*M* + H]⁺, 319.1917; found, 319.1921.

N-(4-Ethylcyclohexyl)-2-(pyridin-3-yl)quinazolin-4-amine (*cis/trans* = 3/2) (**6b**). Pale-yellow solid (38 mg, 30%); mp 62–65 °C. *Cis* isomer: ¹H NMR (500 MHz, CDCl₃) δ 9.74 (s, 1H), 8.81 (d, *J* = 7.7 Hz, 1H), 8.68 (s, 1H), 7.92 (d, *J* = 8.2 Hz, 1H), 7.77–7.71 (m, 1H), 7.48–7.39 (m, 2H), 5.85 (d, *J* = 5.8 Hz, 1H), 4.67–4.61 (m, 1H), 2.02–1.70 (m, 5H), 1.38–1.15 (m, 4H), 0.93 (t, *J* = 7.4 Hz, 3H). ¹³C NMR (125 MHz, CDCl₃) δ 159.0, 158.8, 150.8, 150.4, 135.8, 134.5, 132.8, 128.9, 125.9, 123.3, 120.5, 113.9, 47.5, 39.0, 30.8, 29.7, 29.3, 28.1, 11.8. *Trans* isomer: ¹H NMR (500 MHz, CDCl₃) δ 9.74 (s, 1H), 8.81 (d, *J* = 7.7 Hz, 1H), 8.68 (s, 1H), 7.92 (d, *J* = 8.2 Hz, 1H), 7.77–7.71 (m, 1H), 7.48–7.39 (m, 2H), 5.63 (brs, 1H), 4.38–4.30 (m, 1H), 2.28 (d, *J* = 9.9 Hz, 2H), 1.99–1.70 (m, 2H), 1.54–1.40 (m, 1H), 1.40–1.30 (m, 2H), 1.30–1.15 (m, 2H), 0.93 (t, *J* = 7.4 Hz, 3H). ¹³C NMR (125 MHz, CDCl₃) δ 159.1, 158.8, 150.8, 150.4, 135.8, 134.5, 132.8, 129.0, 125.9, 123.3, 120.7, 114.0, 50.8, 37.7, 33.1, 31.7, 28.3, 11.8. HRMS (ESI): calcd for C₂₁H₂₅N₄ [*M* + H]⁺, 333.2074; found, 333.2080.

Trans-N-(4-Methylcyclohexyl)-2-(pyridin-3-yl)quinazolin-4-amine (**6c**). White solid (52 mg, 55%); mp 173–175 °C. ¹H NMR (500 MHz, CDCl₃) δ 9.75 (s, 1H), 8.80 (d, *J* = 7.8 Hz, 1H), 8.69 (s, 1H), 7.92 (d, *J* = 8.3 Hz, 1H), 7.77–7.71 (m, 1H), 7.70 (d, *J* = 8.2 Hz, 1H), 7.53–7.33 (m, 2H), 5.63 (d, *J* = 5.3 Hz, 1H), 4.38–4.26 (m, 1H), 2.28 (d, *J* = 9.9 Hz, 2H), 1.84 (d, *J* = 12.6 Hz, 2H), 1.54–1.40 (m, 1H), 1.40–1.30 (m, 2H), 1.30–1.14 (m, 2H), 0.98 (d, *J* = 6.5 Hz, 3H). ¹³C NMR (125 MHz, CDCl₃) δ 159.0, 158.8, 150.8, 150.5, 150.4, 135.7, 134.6, 132.7, 129.0, 125.7, 123.2, 120.5, 113.9, 50.4, 34.1, 33.1, 32.3, 22.3. HRMS (ESI): calcd for C₂₀H₂₃N₄ [*M* + H]⁺, 319.1917; found, 319.1921.

N-(4-Methoxycyclohexyl)-2-(pyridin-3-yl)quinazolin-4-amine (**6d**). White solid (50 mg, 50%); mp 163–165 °C. ¹H NMR (500 MHz, CDCl₃) δ 9.73 (s, 1H), 8.81 (d, *J* = 7.7 Hz, 1H), 8.70 (d, *J* = 3.4

Table 6. GCase Inhibitory Activity of 9a, 9b, 9c, 11d, 11f, and 11g at pH 5.0, pH 5.9, and pH 7.0, Respectively^a

Comp	Structure	IC ₅₀ (nM)		
		pH 5.0	pH 5.9	pH 7.0
9a		22.4 ± 3.4	8.7 ± 1.1	16.9 ± 2.7
9b		30.1 ± 4.5	9.9 ± 1.3	18.8 ± 2.5
9c		25.9 ± 3.9	8.3 ± 1.0	12.7 ± 1.4
11d		10.5 ± 1.5	6.5 ± 0.7	9.4 ± 1.4
11f		13.9 ± 1.9	8.2 ± 1.0	12.9 ± 2.0
11g		8.9 ± 1.3	5.2 ± 0.6	6.6 ± 1.0

^aExperiments were performed in triplicate, and the mean ± SD is shown.

Hz, 1H), 7.95 (d, J = 8.2 Hz, 1H), 7.81–7.57 (m, 2H), 7.52–7.32 (m, 2H), 5.69 (d, J = 0.8 Hz, 1H), 4.52–4.27 (m, 1H), 3.40 (s, 3H), 3.31–3.13 (m, 1H), 2.35 (d, J = 12.5 Hz, 2H), 2.18 (d, J = 11.3 Hz, 2H), 1.61–1.22 (m, 4H). ¹³C NMR (125 MHz, CDCl₃) δ 159.1, 158.7, 150.8, 150.3, 135.8, 134.3, 132.8, 128.9, 125.9, 123.3, 120.6, 113.8, 78.4, 56.0, 49.7, 30.6, 30.4. HRMS (ESI): calcd for C₂₀H₂₃N₄O [M + H]⁺, 335.1866; found, 335.1866.

N-(4,4-Dimethylcyclohexyl)-2-(pyridin-3-yl)quinazolin-4-amine (6e). White solid (65 mg, 65%); mp 171–172 °C. ¹H NMR (500 MHz, CDCl₃) δ 9.74 (s, 1H), 8.80 (d, J = 7.9 Hz, 1H), 8.69 (d, J = 3.7 Hz, 1H), 7.90 (s, 1H), 7.79–7.63 (m, 2H), 7.45 (s, 1H), 7.41 (d, J = 3.1 Hz, 1H), 5.66 (d, J = 5.5 Hz, 1H), 4.43–4.25 (m, 1H), 2.16–2.00 (m, 2H), 1.64–1.38 (m, 6H), 1.01 (d, J = 3.0 Hz, 6H). ¹³C NMR (125 MHz, CDCl₃) δ 159.0, 158.8, 150.8, 150.4, 135.7, 134.5, 132.7, 129.0,

125.8, 123.2, 120.6, 113.9, 50.3, 37.9, 31.8, 29.9, 28.7, 25.2. HRMS (ESI): calcd for C₂₁H₂₅N₄ [M + H]⁺, 333.2074; found, 333.2076.

N-(4,4-Difluorocyclohexyl)-2-(pyridin-3-yl)quinazolin-4-amine (6f). White solid (52 mg, 51%); mp 196–197 °C. ¹H NMR (500 MHz, CDCl₃) δ 9.72 (s, 1H), 8.80 (d, J = 7.8 Hz, 1H), 8.70 (d, J = 2.6 Hz, 1H), 7.95 (d, J = 8.3 Hz, 1H), 7.80–7.75 (m, 1H), 7.73 (d, J = 8.1 Hz, 1H), 7.47 (t, J = 7.5 Hz, 1H), 7.43 (dd, J = 7.7, 4.8 Hz, 1H), 5.70 (d, J = 6.2 Hz, 1H), 4.60–4.45 (m, 1H), 2.32 (d, J = 12.6 Hz, 2H), 2.28–2.12 (m, 2H), 2.12–1.93 (m, 2H), 1.85–1.70 (m, 2H). ¹³C NMR (125 MHz, CDCl₃) δ 159.1, 158.5, 150.8, 150.3, 150.1, 135.8, 134.3, 133.1, 129.0, 126.2, 123.6 (q, J_{C-F} = 241 Hz), 123.4, 120.5, 113.8, 48.1, 32.5 (t, J_{C-F} = 24.7 Hz), 28.6 (d, J_{C-F} = 9.2 Hz). HRMS (ESI): calcd for C₁₉H₁₉F₂N₄ [M + H]⁺, 341.1572; found, 341.1577.

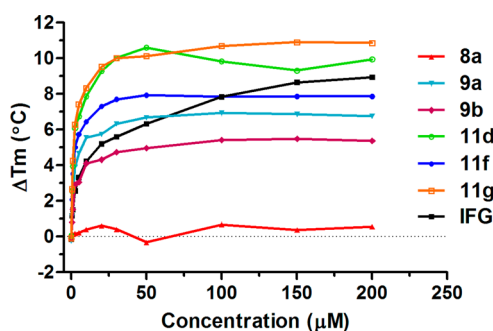


Figure 3. Fluorescent thermal shift analysis of selected compounds. Compound 9a, 9b, 11d, 11f, 11g, and IFG showed their ability to stabilize wild-type GCase in a dose-dependent manner. Data represent the results of three independent experiments performed with three replicates per sample.

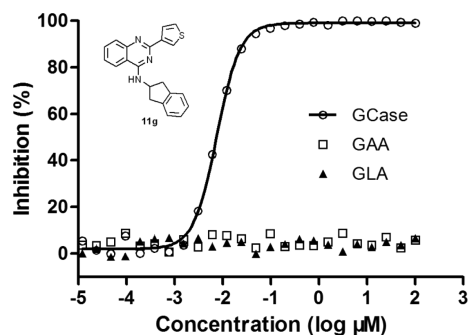


Figure 4. Selectivity of inhibitor 11g with related hydrolases. 11g was tested on GCase, acid α -glucosidase (GAA), and α -galactosidase A (GLA). Data represent the results of three independent experiments performed with three replicates per sample.

N-(4-Dimethylaminocyclohexyl)-2-(pyridin-3-yl)quinazolin-4-amine (**6g**). Pale-yellow solid (63 mg, 60%); mp 231–235 °C. ^1H NMR (500 MHz, CDCl_3) δ 9.70 (s, 1H), 8.76 (d, J = 7.8 Hz, 1H), 8.65 (d, J = 3.6 Hz, 1H), 7.87 (d, J = 8.2 Hz, 1H), 7.78 (d, J = 8.1 Hz, 1H), 7.75–7.66 (m, 1H), 7.42 (t, J = 7.5 Hz, 1H), 7.37 (dd, J = 7.5, 4.9 Hz, 1H), 6.02 (d, J = 6.7 Hz, 1H), 4.64 (s, 1H), 2.38 (s, 6H), 2.30 (s, 1H), 2.05 (s, 2H), 1.83 (s, 6H). ^{13}C NMR (125 MHz, CDCl_3) δ 159.0, 158.6, 150.6, 150.3, 150.2, 135.7, 134.6, 132.7, 128.8, 125.9, 123.2, 120.8, 114.0, 62.2, 46.0, 42.5, 27.9, 25.6. HRMS (ESI): calcd for $\text{C}_{21}\text{H}_{26}\text{N}_5$ $[\text{M} + \text{H}]^+$, 348.2183; found, 348.2184.

N-(Tetrahydro-2H-pyran-3-yl)-2-(pyridin-3-yl)quinazolin-4-amine (**6h**). White solid (48 mg, 53%); mp 112–113 °C. ^1H NMR (500 MHz, CDCl_3) δ 9.72 (s, 1H), 8.80 (dt, J = 7.9, 1.9 Hz, 1H), 8.68 (d, J = 3.7 Hz, 1H), 7.93 (d, J = 8.3 Hz, 1H), 7.80 (d, J = 8.2 Hz, 1H), 7.78–7.73 (m, 1H), 7.50–7.44 (m, 1H), 7.41 (dd, J = 7.8, 4.8 Hz, 1H), 6.18 (d, J = 7.1 Hz, 1H), 4.68–4.59 (m, 1H), 4.01 (dd, J = 11.5, 2.7 Hz, 1H), 3.89–3.80 (m, 1H), 3.80–3.66 (m, 2H), 2.08–2.00 (m, 3H), 1.95–1.83 (m, 1H), 1.73–1.61 (m, 1H). ^{13}C NMR (125 MHz, CDCl_3) δ 159.0, 158.6, 150.7, 150.3, 150.2, 135.9, 134.4, 133.0, 128.9, 126.1, 123.3, 120.7, 113.9, 71.5, 68.6, 46.5, 27.8, 23.0. HRMS (ESI): calcd for $\text{C}_{18}\text{H}_{19}\text{N}_4\text{O}$ $[\text{M} + \text{H}]^+$, 307.1553; found, 307.1556.

N-(1-Methylpiperidin-4-yl)-2-(pyridin-3-yl)quinazolin-4-amine (**6i**). Pale-yellow solid (34 mg, 35%); mp 132–133 °C. ^1H NMR (500 MHz, CDCl_3) δ 9.72 (s, 1H), 8.78 (d, J = 7.5 Hz, 1H), 8.68 (d, J = 3.4 Hz, 1H), 7.90 (d, J = 8.1 Hz, 1H), 7.73 (t, J = 7.4 Hz, 1H), 7.49–7.34 (m, 3H), 5.73 (d, J = 6.1 Hz, 1H), 4.48–4.30 (m, 1H), 2.91 (d, J = 9.1 Hz, 2H), 2.36 (s, 3H), 2.32–2.17 (m, 4H), 1.72 (m, 2H). ^{13}C NMR (125 MHz, CDCl_3) δ 159.0, 158.7, 150.8, 150.4, 150.3, 135.6, 134.5, 132.8, 129.0, 125.9, 123.2, 120.7, 113.9, 54.7, 48.0, 46.3, 32.1. HRMS (ESI): calcd for $\text{C}_{19}\text{H}_{22}\text{N}_5$ $[\text{M} + \text{H}]^+$, 320.1870; found, 320.1872.

N-(1-Isopropylpiperidin-4-yl)-2-(pyridin-3-yl)quinazolin-4-amine (**6j**). Yellow solid (49 mg, 47%); mp 191–192 °C. ^1H NMR (500 MHz, CDCl_3) δ 9.73 (d, J = 1.2 Hz, 1H), 8.79 (dt, J = 7.8, 1.5 Hz,

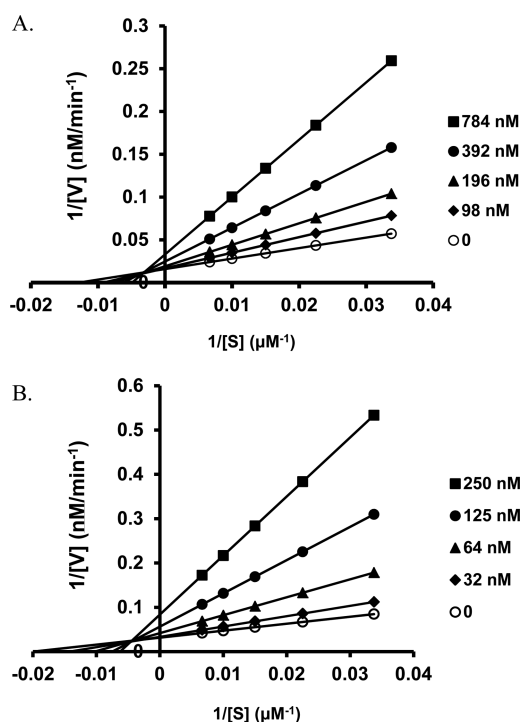


Figure 5. Lineweaver–Burk plots of the enzyme kinetics of GCase inhibitors (A) 4 and (B) 11g. Each inhibitor was tested in triplicate in two independent assays at the concentrations shown in the legend box of each graph, with (○) indicating the absence of inhibitor. (A) Compounds 4 and (B) 11g showed an increase in K_m and a decrease in V_{max} indicating linear mixed inhibition.

1H), 8.68 (dd, J = 4.6, 1.2 Hz, 1H), 7.91 (d, J = 8.3 Hz, 1H), 7.77–7.73 (m, 1H), 7.71 (d, J = 8.2 Hz, 1H), 7.49–7.43 (m, 1H), 7.41 (dd, J = 7.8, 4.8 Hz, 1H), 5.68 (d, J = 7.1 Hz, 1H), 4.49–4.35 (m, 1H), 2.99 (d, J = 11.1 Hz, 2H), 2.90–2.79 (m, 1H), 2.47 (t, J = 11.6 Hz, 2H), 2.28 (d, J = 11.5 Hz, 2H), 1.80–1.66 (m, 2H), 1.13 (d, J = 6.4 Hz, 6H). ^{13}C NMR (125 MHz, CDCl_3) δ 159.0, 158.7, 150.8, 150.5, 150.4, 135.7, 134.5, 132.8, 129.0, 125.9, 123.3, 120.6, 113.9, 54.9, 48.7, 47.8, 32.3, 18.4. HRMS (ESI): calcd for $\text{C}_{21}\text{H}_{26}\text{N}_5$ $[\text{M} + \text{H}]^+$, 348.2183; found, 348.2184.

N-(1-Benzylpiperidin-4-yl)-2-(pyridin-3-yl)quinazolin-4-amine (**6k**). Yellow solid (67 mg, 57%); mp 180–182 °C. ^1H NMR (500 MHz, CDCl_3) δ 9.72 (d, J = 1.6 Hz, 1H), 8.78 (dt, J = 7.9, 1.9 Hz, 1H), 8.69 (dd, J = 4.8, 1.6 Hz, 1H), 7.91 (d, J = 8.2 Hz, 1H), 7.77–7.72 (m, 1H), 7.71 (d, J = 8.1 Hz, 1H), 7.50–7.43 (m, 1H), 7.41 (dd, J = 7.8, 5.0 Hz, 1H), 7.39–7.27 (m, 5H), 5.66 (d, J = 7.1 Hz, 1H), 4.49–4.37 (m, 1H), 3.62 (s, 2H), 2.98 (d, J = 10.6 Hz, 2H), 2.38–2.29 (m, 2H), 2.24 (d, J = 11.4 Hz, 2H), 1.81–1.69 (m, 2H). ^{13}C NMR (125 MHz, CDCl_3) δ 159.0, 158.7, 150.8, 150.5, 150.3, 135.6, 134.5, 132.8, 129.4, 129.0, 128.4, 127.4, 125.9, 123.2, 120.6, 113.9, 63.2, 52.5, 48.4, 32.0. HRMS (ESI): calcd for $\text{C}_{25}\text{H}_{26}\text{N}_5$ $[\text{M} + \text{H}]^+$, 396.2183; found, 396.2184.

N-Cyclooctyl-2-(pyridin-3-yl)quinazolin-4-amine (**7a**). White solid (65 mg, 66%); mp 140–142 °C. ^1H NMR (500 MHz, CDCl_3) δ 9.75 (d, J = 1.4 Hz, 1H), 8.82 (d, J = 7.9 Hz, 1H), 8.69 (dd, J = 4.7, 1.4 Hz, 1H), 7.92 (d, J = 8.3 Hz, 1H), 7.76–7.72 (m, 1H), 7.70 (d, J = 8.1 Hz, 1H), 7.51–7.35 (m, 2H), 5.73 (d, J = 6.2 Hz, 1H), 4.73–4.56 (m, 1H), 2.18–2.00 (m, 2H), 2.00–1.43 (m, 12H). ^{13}C NMR (125 MHz, CDCl_3) δ 158.8, 158.6, 150.7, 150.3, 150.2, 135.8, 134.5, 132.7, 128.9, 125.8, 123.3, 120.5, 114.0, 51.0, 32.7, 27.2, 26.1, 24.2. HRMS (ESI): calcd for $\text{C}_{21}\text{H}_{25}\text{N}_4$ $[\text{M} + \text{H}]^+$, 333.2074; found, 333.2076.

N-Cycloheptyl-2-(pyridin-3-yl)quinazolin-4-amine (**7b**). Off-white solid (70 mg, 74%); mp 158–159 °C. ^1H NMR (500 MHz, CDCl_3) δ 9.75 (s, 1H), 8.82 (d, J = 7.9 Hz, 1H), 8.68 (s, 1H), 7.93 (d, J = 8.3 Hz, 1H), 7.78–7.65 (m, 2H), 7.50–7.37 (m, 2H), 5.76 (d, J = 5.6 Hz, 1H), 4.64–4.46 (m, 1H), 2.25–2.12 (m, 2H), 1.83–1.52 (m, 10H).

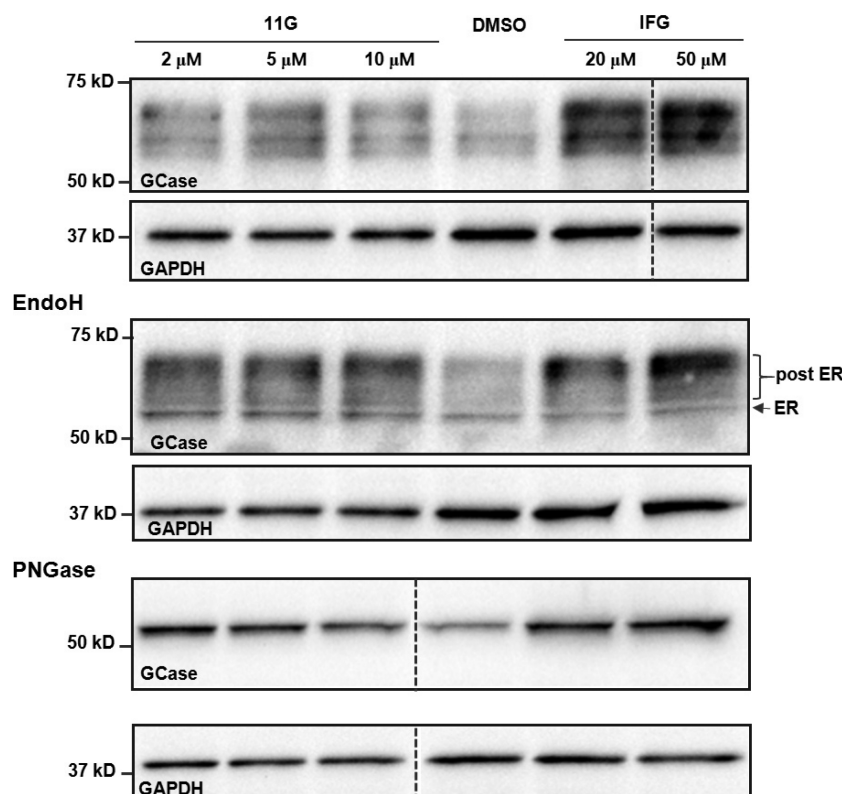


Figure 6. Modulator **11g** increases GCase protein levels in patient-derived Gaucher's disease fibroblasts. Top: Western blot of N370S fibroblast treated with **11g** or IFG for 3 days. Middle: Western blot of endoH digestion of N370S fibroblast after a 3-day treatment of **11g**, IFG, or DMSO; endoH resistance of proteins indicates their post-ER localization; Bottom: Western blot of PNGase F digestion of N370S fibroblast after a 3-day treatment of **11g**, IFG, or DMSO. The GAPDH signal was used for the loading control.

^{13}C NMR (125 MHz, CDCl_3) δ 158.7, 158.6, 150.7, 150.3, 150.2, 135.8, 134.5, 132.7, 128.8, 125.9, 123.3, 120.6, 113.9, 52.3, 34.9, 28.3, 24.6. HRMS (ESI): calcd for $\text{C}_{20}\text{H}_{23}\text{N}_4$ $[\text{M} + \text{H}]^+$, 319.1917; found, 319.1918.

N-Cyclopentyl-2-(pyridin-3-yl)quinazolin-4-amine (7c). Off-white solid (52 mg, 60%); mp 147–148 °C. ^1H NMR (500 MHz, CDCl_3) δ 9.76 (d, J = 1.5 Hz, 1H), 8.81 (dt, J = 7.9, 1.9 Hz, 1H), 8.68 (dd, J = 4.8, 1.7 Hz, 1H), 7.91 (d, J = 8.2 Hz, 1H), 7.76–7.71 (m, 1H), 7.70 (d, J = 8.2 Hz, 1H), 7.46–7.42 (m, 1H), 7.40 (dd, J = 7.9, 4.8 Hz, 1H), 5.73 (d, J = 6.1 Hz, 1H), 4.80–4.72 (m, 1H), 2.34–2.25 (m, 2H), 1.86–1.71 (m, 4H), 1.67–1.59 (m, 2H). ^{13}C NMR (125 MHz, CDCl_3) δ 159.4, 158.8, 150.7, 150.4, 150.3, 135.7, 134.6, 132.7, 129.0, 125.8, 123.2, 120.6, 113.9, 53.2, 33.4, 24.1. HRMS (ESI): calcd for $\text{C}_{18}\text{H}_{19}\text{N}_4$ $[\text{M} + \text{H}]^+$, 291.1604; found, 291.1604.

N-Cyclobutyl-2-(pyridin-3-yl)quinazolin-4-amine (7d). Off-white solid (47 mg, 57%); mp 173–174 °C. ^1H NMR (500 MHz, CDCl_3) δ 9.75 (s, 1H), 8.87–8.79 (m, 1H), 8.69 (d, J = 4.2 Hz, 1H), 7.93 (dd, J = 8.0, 4.1 Hz, 1H), 7.74 (t, J = 8.2 Hz, 2H), 7.47–7.43 (m, 1H), 7.43–7.39 (m, 1H), 6.03 (s, 1H), 4.96–4.97 (m, 1H), 2.66–2.54 (m, 2H), 2.16–2.03 (m, 2H), 1.96–1.85 (m, 2H). ^{13}C NMR (125 MHz, CDCl_3) δ 158.8, 150.7, 150.5, 150.4, 135.7, 134.5, 132.8, 129.0, 125.9, 123.2, 120.6, 113.7, 46.8, 31.4, 15.6. HRMS (ESI): calcd for $\text{C}_{17}\text{H}_{17}\text{N}_4$ $[\text{M} + \text{H}]^+$, 277.1448; found, 277.1449.

N-Cyclopropyl-2-(pyridin-3-yl)quinazolin-4-amine (7e). Pale-yellow solid (30 mg, 38%); mp 180–181 °C. ^1H NMR (500 MHz, CDCl_3) δ 9.81 (s, 1H), 8.89 (d, J = 7.9 Hz, 1H), 8.70 (d, J = 3.7 Hz, 1H), 7.96 (d, J = 8.3 Hz, 1H), 7.77–7.73 (m, 1H), 7.71 (d, J = 8.2 Hz, 1H), 7.47–7.36 (m, 2H), 6.14 (s, 1H), 3.17 (td, J = 6.9, 3.1 Hz, 1H), 1.07–0.95 (m, 2H), 0.79–0.67 (m, 2H). ^{13}C NMR (125 MHz, CDCl_3) δ 160.9, 158.9, 150.8, 150.5, 150.4, 135.8, 134.5, 132.8, 129.0, 126.0, 123.2, 120.6, 113.9, 24.5, 7.5. HRMS (ESI): calcd for $\text{C}_{16}\text{H}_{15}\text{N}_4$ $[\text{M} + \text{H}]^+$, 263.1291; found, 263.1291.

N-(Adamantan-1-yl)-2-(pyridin-3-yl)quinazolin-4-amine (7f). White solid (37 mg, 35%); mp 114–116 °C. ^1H NMR (500 MHz,

CDCl_3) δ 9.73 (d, J = 1.6 Hz, 1H), 8.83 (d, J = 7.8 Hz, 1H), 8.69 (dd, J = 4.7, 1.5 Hz, 1H), 7.92 (d, J = 8.1 Hz, 1H), 7.80–7.69 (m, 1H), 7.66 (d, J = 8.1 Hz, 1H), 7.51–7.32 (m, 2H), 5.58 (s, 1H), 2.38 (d, J = 2.3 Hz, 6H), 2.25–2.18 (m, 3H), 1.88–1.74 (m, 6H). ^{13}C NMR (125 MHz, CDCl_3) δ 159.0, 158.1, 150.7, 150.3, 135.8, 134.5, 132.6, 128.9, 125.9, 123.3, 120.6, 114.2, 53.6, 41.7, 36.7, 29.7. HRMS (ESI): calcd for $\text{C}_{23}\text{H}_{25}\text{N}_4$ $[\text{M} + \text{H}]^+$, 357.2074; found, 357.2074.

N-(Bicyclo[2.2.1]heptan-2-yl)-2-(pyridin-3-yl)quinazolin-4-amine (7g). White solid (47 mg, 50%); mp 145–146 °C. ^1H NMR (500 MHz, CDCl_3) δ 9.75 (s, 1H), 8.82 (dt, J = 7.9, 1.8 Hz, 1H), 8.68 (d, J = 3.9 Hz, 1H), 7.91 (d, J = 8.3 Hz, 1H), 7.75–7.71 (m, 1H), 7.69 (d, J = 8.2 Hz, 1H), 7.49–7.35 (m, 2H), 5.64 (d, J = 5.5 Hz, 1H), 4.27–4.16 (m, 1H), 2.51 (d, J = 4.1 Hz, 1H), 2.39 (s, 1H), 2.05 (ddd, J = 13.2, 7.9, 2.2 Hz, 1H), 1.73–1.61 (m, 1H), 1.61–1.53 (m, 1H), 1.51 (d, J = 10.1 Hz, 1H), 1.48–1.36 (m, 2H), 1.34–1.20 (m, 2H). ^{13}C NMR (125 MHz, CDCl_3) δ 158.9, 158.7, 150.7, 150.3, 150.2, 135.8, 134.5, 132.7, 128.9, 125.8, 123.3, 120.5, 113.9, 55.1, 42.1, 41.0, 36.0, 35.9, 28.3, 26.7. HRMS (ESI): calcd for $\text{C}_{20}\text{H}_{21}\text{N}_4$ $[\text{M} + \text{H}]^+$, 317.1761; found, 317.1763.

N-(Cyclohexylmethyl)-2-(pyridin-3-yl)quinazolin-4-amine (7h). Pale-yellow solid (67 mg, 71%); mp 121–123 °C. ^1H NMR (500 MHz, CDCl_3) δ 9.75 (s, 1H), 8.81 (d, J = 7.8 Hz, 1H), 8.68 (d, J = 3.8 Hz, 1H), 7.91 (d, J = 8.2 Hz, 1H), 7.79–7.65 (m, 2H), 7.50–7.34 (m, 2H), 5.98 (s, 1H), 3.65 (t, J = 6.1 Hz, 2H), 1.87 (d, J = 12.6 Hz, 2H), 1.82–1.61 (m, 4H), 1.32–1.18 (m, 3H), 1.14–1.04 (m, 1H). ^{13}C NMR (125 MHz, CDCl_3) δ 159.9, 158.8, 150.7, 150.3, 135.7, 134.6, 132.7, 128.9, 125.8, 123.2, 120.5, 114.0, 47.6, 38.0, 31.3, 26.5, 26.0. HRMS (ESI): calcd for $\text{C}_{20}\text{H}_{23}\text{N}_4$ $[\text{M} + \text{H}]^+$, 319.1917; found, 319.1920.

N-(2-Cyclohexylethyl)-2-(pyridin-3-yl)quinazolin-4-amine (7i). White solid (48 mg, 48%); mp 153–154 °C. ^1H NMR (500 MHz, CDCl_3) δ 9.76 (s, 1H), 8.86–8.78 (m, 1H), 8.69 (d, J = 4.1 Hz, 1H), 7.92 (dd, J = 7.9, 5.4 Hz, 1H), 7.79–7.67 (m, 2H), 7.48–7.37 (m, 2H), 5.84 (s, 1H), 3.86–3.75 (m, 2H), 1.83 (d, J = 12.3 Hz, 2H),

1.76–1.60 (m, 5H), 1.50–1.38 (m, 1H), 1.33–1.12 (m, 3H), 1.08–0.96 (m, 2H). ^{13}C NMR (125 MHz, CDCl_3) δ 159.7, 158.8, 150.7, 150.4, 150.3, 135.8, 135.7, 134.5, 132.8, 132.7, 128.9, 128.9, 125.9, 123.2, 120.6, 114.0, 39.4, 37.0, 35.7, 33.4, 26.6, 26.3. HRMS (ESI): calcd for $\text{C}_{21}\text{H}_{25}\text{N}_4$ $[\text{M} + \text{H}]^+$, 333.2074; found, 333.2074.

N-Phenyl-2-(pyridin-3-yl)quinazolin-4-amine (8a). Off-white solid (55 mg, 62%); mp 179–180 °C. ^1H NMR (500 MHz, CDCl_3) δ 9.73 (d, J = 1.8 Hz, 1H), 8.82 (dt, J = 7.9, 1.9 Hz, 1H), 8.70 (dd, J = 4.8, 1.6 Hz, 1H), 8.01 (d, J = 8.3 Hz, 1H), 7.95 (d, J = 8.1 Hz, 1H), 7.86 (d, J = 7.6 Hz, 2H), 7.84–7.80 (m, 1H), 7.69 (brs, 1H), 7.61–7.52 (m, 1H), 7.50–7.45 (m, 2H), 7.43 (dd, J = 7.9, 4.8 Hz, 1H), 7.21 (t, J = 7.4 Hz, 1H). ^{13}C NMR (125 MHz, CDCl_3) δ 158.4, 157.6, 150.8, 150.7, 150.2, 138.4, 136.1, 134.2, 133.3, 129.3, 129.2, 126.8, 124.6, 123.4, 121.6, 120.5, 114.1. HRMS (ESI): calcd for $\text{C}_{19}\text{H}_{15}\text{N}_4$ $[\text{M} + \text{H}]^+$, 299.1291; found, 299.1292.

N-Benzyl-2-(pyridin-3-yl)quinazolin-4-amine (8b). Off-white solid (65 mg, 70%); mp 140–141 °C. ^1H NMR (500 MHz, CDCl_3) δ 9.56 (s, 1H), 8.61 (d, J = 7.9 Hz, 1H), 8.47 (d, J = 3.6 Hz, 1H), 7.74 (d, J = 8.3 Hz, 1H), 7.61 (d, J = 8.2 Hz, 1H), 7.58–7.44 (m, 1H), 7.28–7.18 (m, 4H), 7.18–7.13 (m, 2H), 7.13–7.07 (m, 1H), 6.39 (s, 1H), 4.78 (d, J = 5.4 Hz, 2H). ^{13}C NMR (125 MHz, CDCl_3) δ 159.6, 158.7, 150.6, 150.4, 150.2, 138.5, 135.8, 134.5, 132.8, 128.8, 128.0, 127.7, 126.0, 123.2, 120.9, 113.9, 45.4. HRMS (ESI): calcd for $\text{C}_{20}\text{H}_{17}\text{N}_4$ $[\text{M} + \text{H}]^+$, 313.1448; found, 313.1453.

N-Phenethyl-2-(pyridin-3-yl)quinazolin-4-amine (8c). White solid (43 mg, 44%); mp 140–141 °C. ^1H NMR (500 MHz, CDCl_3) δ 9.79 (s, 1H), 8.85 (d, J = 7.1 Hz, 1H), 8.70 (s, 1H), 7.94 (d, J = 8.4 Hz, 1H), 7.78–7.69 (m, 1H), 7.60 (d, J = 8.0 Hz, 1H), 7.46–7.39 (m, 2H), 7.38–7.31 (m, 2H), 7.30–7.25 (m, 3H), 5.98 (s, 1H), 4.11–3.99 (m, 2H), 3.11 (t, J = 6.9 Hz, 2H). ^{13}C NMR (125 MHz, CDCl_3) δ 159.6, 158.7, 150.8, 150.3, 150.2, 139.0, 135.8, 134.4, 132.9, 129.0, 128.9, 126.8, 126.0, 123.3, 120.5, 113.9, 42.6, 35.4. HRMS (ESI): calcd for $\text{C}_{21}\text{H}_{19}\text{N}_4$ $[\text{M} + \text{H}]^+$, 327.1604; found, 327.1603.

N-(3-Phenylpropyl)-2-(pyridin-3-yl)quinazolin-4-amine (8d). Off-white sticky oil (60 mg, 59%). ^1H NMR (500 MHz, CDCl_3) δ 9.74 (s, 1H), 8.76 (dt, J = 7.9, 1.8 Hz, 1H), 8.68 (d, J = 3.6 Hz, 1H), 7.90 (d, J = 8.3 Hz, 1H), 7.78–7.66 (m, 1H), 7.53 (d, J = 7.8 Hz, 1H), 7.45–7.34 (m, 2H), 7.33–7.27 (m, 2H), 7.25–7.19 (m, 3H), 5.94 (s, 1H), 3.89–3.75 (m, 2H), 2.81 (t, J = 7.4 Hz, 2H), 2.13 (p, J = 7.2 Hz, 2H). ^{13}C NMR (125 MHz, CDCl_3) δ 159.7, 158.7, 150.7, 150.3, 150.2, 141.6, 135.8, 134.5, 132.7, 128.8, 128.7, 128.5, 126.2, 125.8, 123.2, 120.6, 113.9, 41.2, 33.7, 30.7. HRMS (ESI): calcd for $\text{C}_{22}\text{H}_{21}\text{N}_4$ $[\text{M} + \text{H}]^+$, 341.1761; found, 341.1758.

N-(4-Phenylbutyl)-2-(pyridin-3-yl)quinazolin-4-amine (8e). Pale-yellow solid (73 mg, 69%); mp 108–109 °C. ^1H NMR (500 MHz, CDCl_3) δ 9.75 (s, 1H), 8.81 (d, J = 7.9 Hz, 1H), 8.69 (d, J = 3.7 Hz, 1H), 7.93 (d, J = 8.3 Hz, 1H), 7.77–7.71 (m, 1H), 7.70 (d, J = 8.1 Hz, 1H), 7.51–7.35 (m, 2H), 7.28 (d, J = 7.7 Hz, 2H), 7.23–7.10 (m, 3H), 5.90 (s, 1H), 3.89–3.70 (m, 2H), 2.72 (t, J = 6.7 Hz, 2H), 1.90–1.75 (m, 4H). ^{13}C NMR (125 MHz, CDCl_3) δ 159.7, 158.7, 150.8, 150.3, 150.1, 142.1, 135.8, 134.4, 132.8, 128.8, 128.5, 128.5, 126.0, 125.9, 123.3, 120.6, 113.9, 41.4, 35.7, 29.0, 28.9. HRMS (ESI): calcd for $\text{C}_{23}\text{H}_{23}\text{N}_4$ $[\text{M} + \text{H}]^+$, 355.1917; found, 355.1919.

N-(2-(Pyridin-2-yl)ethyl)-2-(pyridin-3-yl)quinazolin-4-amine (8f). White solid (57 mg, 58%); mp 138–139 °C. ^1H NMR (500 MHz, CDCl_3) δ 9.75 (d, J = 1.2 Hz, 1H), 8.82 (dt, J = 7.9, 1.9 Hz, 1H), 8.70–8.66 (m, 1H), 8.51 (s, 1H), 8.47 (d, J = 4.1 Hz, 1H), 7.93 (d, J = 8.2 Hz, 1H), 7.77–7.72 (m, 1H), 7.68 (d, J = 8.1 Hz, 1H), 7.59 (d, J = 7.8 Hz, 1H), 7.46–7.38 (m, 2H), 7.24 (dd, J = 7.7, 4.9 Hz, 1H), 6.28 (t, J = 5.3 Hz, 1H), 4.10–3.96 (m, 2H), 3.13 (t, J = 7.0 Hz, 2H). ^{13}C NMR (125 MHz, CDCl_3) δ 159.7, 158.6, 150.7, 150.2, 150.1, 148.1, 136.6, 135.8, 134.7, 134.4, 133.0, 128.9, 126.2, 123.8, 123.4, 120.7, 113.9, 42.4, 32.6. HRMS (ESI): calcd for $\text{C}_{20}\text{H}_{18}\text{N}_5$ $[\text{M} + \text{H}]^+$, 328.1557; found, 328.1561.

N-(2-(Pyridin-3-yl)ethyl)-2-(pyridin-3-yl)quinazolin-4-amine (8g). Off-white solid (67 mg, 68%); mp 102–104 °C. ^1H NMR (500 MHz, CDCl_3) δ 9.77 (d, J = 1.4 Hz, 1H), 8.83 (dt, J = 7.9, 1.9 Hz, 1H), 8.68 (dd, J = 4.8, 1.7 Hz, 1H), 7.91 (d, J = 8.0 Hz, 1H), 7.73 (ddd, J = 8.3, 7.0, 1.3 Hz, 1H), 7.57 (d, J = 7.8 Hz, 1H), 7.46–7.37 (m, 2H), 7.07 (d, J = 8.3 Hz, 2H), 6.72–6.62 (m, 2H), 5.96–5.87 (m, 1H), 4.03–3.94

(m, 2H), 2.98 (t, J = 6.9 Hz, 2H). ^{13}C NMR (125 MHz, CDCl_3) δ 159.6, 158.8, 150.7, 150.3, 145.1, 135.8, 134.5, 132.8, 129.8, 128.9, 128.8, 125.9, 123.3, 120.6, 115.6, 114.0, 42.8, 34.5. HRMS (ESI): calcd for $\text{C}_{20}\text{H}_{18}\text{N}_5$ $[\text{M} + \text{H}]^+$, 328.1557; found, 328.1560.

(S)-2-(Pyridin-3-yl)-N-(1,2,3,4-tetrahydronaphthalen-2-yl)-quinazolin-4-amine (9a). Off-white solid (74 mg, 70%); mp 150–152 °C. ^1H NMR (500 MHz, CDCl_3) δ 9.75 (s, 1H), 8.82 (d, J = 7.9 Hz, 1H), 8.68 (d, J = 3.7 Hz, 1H), 7.95 (d, J = 8.3 Hz, 1H), 7.75 (t, J = 7.7 Hz, 1H), 7.70 (d, J = 8.1 Hz, 1H), 7.47–7.42 (m, 1H), 7.41 (dd, J = 7.9, 4.8 Hz, 1H), 7.24–7.11 (m, 4H), 5.87 (d, J = 5.2 Hz, 1H), 5.00–4.87 (m, 1H), 3.43 (dd, J = 16.2, 5.0 Hz, 1H), 3.12–2.88 (m, 3H), 2.40–2.30 (m, 1H), 2.13–2.01 (m, 1H). ^{13}C NMR (125 MHz, CDCl_3) δ 159.2, 158.7, 150.8, 150.2, 135.8, 135.7, 134.3, 134.1, 132.9, 129.7, 129.1, 128.9, 126.4, 126.2, 126.0, 123.3, 120.7, 113.9, 47.1, 35.8, 28.5, 27.5. HRMS (ESI): calcd for $\text{C}_{23}\text{H}_{21}\text{N}_4$ $[\text{M} + \text{H}]^+$, 353.1761; found, 328.1762.

(R)-2-(Pyridin-3-yl)-N-(1,2,3,4-tetrahydronaphthalen-2-yl)-quinazolin-4-amine (9b). Off-white solid (65 mg, 62%); mp 153–156 °C. ^1H NMR (500 MHz, CDCl_3) δ 9.75 (s, 1H), 8.82 (d, J = 7.9 Hz, 1H), 8.68 (d, J = 3.7 Hz, 1H), 7.95 (d, J = 8.3 Hz, 1H), 7.75 (t, J = 7.7 Hz, 1H), 7.70 (d, J = 8.1 Hz, 1H), 7.47–7.42 (m, 1H), 7.41 (dd, J = 7.9, 4.8 Hz, 1H), 7.24–7.11 (m, 4H), 5.87 (d, J = 5.2 Hz, 1H), 5.00–4.87 (m, 1H), 3.43 (dd, J = 16.2, 5.0 Hz, 1H), 3.12–2.88 (m, 3H), 2.40–2.30 (m, 1H), 2.13–2.01 (m, 1H). ^{13}C NMR (125 MHz, CDCl_3) δ 159.2, 158.7, 150.8, 150.2, 135.8, 135.7, 134.3, 134.1, 132.9, 129.7, 129.1, 128.9, 126.4, 126.2, 126.0, 123.3, 120.7, 113.9, 47.1, 35.8, 28.5, 27.5. HRMS (ESI): calcd for $\text{C}_{23}\text{H}_{21}\text{N}_4$ $[\text{M} + \text{H}]^+$, 353.1761; found, 328.1764.

N-(2,3-Dihydro-1H-inden-2-yl)-2-(pyridin-3-yl)quinazolin-4-amine (9c). Gray solid (75 mg, 74%); mp 167–168 °C. ^1H NMR (500 MHz, CDCl_3) δ 9.78 (d, J = 1.7 Hz, 1H), 8.84 (dd, J = 7.9, 1.7 Hz, 1H), 8.69 (d, J = 4.7 Hz, 1H), 7.93 (d, J = 8.3 Hz, 1H), 7.77–7.70 (m, 1H), 7.68 (d, J = 8.1 Hz, 1H), 7.47–7.37 (m, 2H), 7.32–7.27 (m, 2H), 7.25–7.20 (m, 2H), 6.04 (s, 1H), 5.37–5.29 (m, 1H), 3.60 (dd, J = 16.2, 7.2 Hz, 2H), 3.08 (dd, J = 16.2, 4.8 Hz, 2H). ^{13}C NMR (125 MHz, CDCl_3) δ 159.4, 158.6, 150.7, 150.3, 141.1, 135.8, 134.4, 132.9, 128.9, 127.0, 126.0, 125.1, 123.3, 120.7, 113.9, 52.6, 40.3. HRMS (ESI): calcd for $\text{C}_{24}\text{H}_{21}\text{NO}$ $[\text{M} + \text{H}]^+$, 339.1618; found, 339.1612.

N-(1,2,3,4-Tetrahydronaphthalen-1-yl)-2-(pyridin-3-yl)quinazolin-4-amine (9d). Pale-yellow sticky oil (35 mg, 33%). ^1H NMR (500 MHz, CDCl_3) δ 9.78 (d, J = 0.9 Hz, 1H), 8.89 (d, J = 7.8 Hz, 1H), 8.69 (d, J = 3.5 Hz, 1H), 8.00 (d, J = 7.8 Hz, 1H), 7.83–7.73 (m, 1H), 7.68 (d, J = 8.0 Hz, 1H), 7.51–7.41 (m, 2H), 7.39 (d, J = 7.6 Hz, 1H), 7.25–7.22 (m, 1H), 7.22–7.15 (m, 2H), 6.02 (s, 1H), 5.94–5.86 (m, 1H), 3.00–2.80 (m, 2H), 2.34–2.23 (m, 1H), 2.20–2.12 (m, 1H), 2.00–1.93 (m, 2H). ^{13}C NMR (125 MHz, CDCl_3) δ 159.0, 158.7, 150.6, 150.2, 138.1, 136.8, 136.1, 133.0, 129.5, 129.1, 128.8, 127.7, 126.6, 126.1, 123.4, 120.7, 113.8, 49.2, 29.6, 29.5, 20.2. HRMS (ESI): calcd for $\text{C}_{23}\text{H}_{21}\text{N}_4$ $[\text{M} + \text{H}]^+$, 353.1761; found, 353.1767.

N-(2,3-Dihydro-1H-inden-1-yl)-2-(pyridin-3-yl)quinazolin-4-amine (9e). Brown solid (57 mg, 56%); mp 128–130 °C. ^1H NMR (500 MHz, CDCl_3) δ 9.78 (d, J = 1.5 Hz, 1H), 8.84 (dt, J = 7.9, 1.9 Hz, 1H), 8.67 (dd, J = 4.8, 1.6 Hz, 1H), 7.95 (d, J = 8.4 Hz, 1H), 7.80–7.73 (m, 1H), 7.70 (d, J = 8.0 Hz, 1H), 7.50–7.37 (m, 3H), 7.35 (d, J = 7.5 Hz, 1H), 7.33–7.28 (m, 1H), 7.26–7.20 (m, 2H), 6.17 (q, J = 7.4 Hz, 1H), 6.02 (d, J = 7.5 Hz, 1H), 3.12 (ddd, J = 15.8, 8.7, 4.0 Hz, 1H), 3.04 (dt, J = 16.0, 8.0 Hz, 1H), 2.92–2.83 (m, 1H), 2.16–2.01 (m, 1H). ^{13}C NMR (125 MHz, CDCl_3) δ 159.5, 158.8, 150.8, 150.5, 150.3, 143.9, 143.4, 135.8, 134.5, 132.9, 129.0, 128.4, 127.0, 126.0, 125.2, 124.3, 123.3, 120.7, 113.8, 56.5, 34.1, 30.5. HRMS (ESI): calcd for $\text{C}_{22}\text{H}_{19}\text{N}_4$ $[\text{M} + \text{H}]^+$, 339.1604; found, 339.1610.

N-(Chroman-3-yl)-2-(pyridin-3-yl)quinazolin-4-amine (9f). White solid (67 mg, 63%); mp 145–148 °C. ^1H NMR (500 MHz, CDCl_3) δ 9.74 (s, 1H), 8.80 (dt, J = 7.9, 1.9 Hz, 1H), 8.68 (d, J = 3.6 Hz, 1H), 7.90 (d, J = 7.9 Hz, 1H), 7.72 (ddd, J = 8.3, 7.0, 1.3 Hz, 1H), 7.63 (d, J = 7.7 Hz, 1H), 7.45–7.34 (m, 2H), 7.19–7.12 (m, 1H), 7.07 (d, J = 6.6 Hz, 1H), 6.95–6.88 (m, 2H), 6.09 (d, J = 7.3 Hz, 1H), 5.11 (ddt, J = 7.3, 3.6, 1.7 Hz, 1H), 4.43 (ddd, J = 11.0, 3.8, 2.2 Hz, 1H), 4.35 (dd, J = 11.0, 1.7 Hz, 1H), 3.34 (dd, J = 16.8, 5.2 Hz, 1H), 3.10 (d, J = 16.8 Hz, 1H). ^{13}C NMR (125 MHz, CDCl_3) δ 159.0, 158.4, 153.9, 150.7,

150.3, 150.1, 135.6, 134.2, 132.9, 130.6, 128.9, 127.8, 126.0, 123.2, 121.5, 120.7, 119.5, 117.0, 113.7, 68.0, 44.0, 30.4. HRMS (ESI): calcd for $C_{22}H_{19}N_4O$ $[M + H]^+$, 355.1553; found, 355.1551.

Preparation of 2-Chloro-N-(2,3-dihydro-1H-inden-2-yl)-quinazolin-4-amine (10). A mixture of 2,4-dichloroquinazoline (398 mg, 2.0 mmol), 2,3-dihydro-1H-inden-2-amine (266 mg, 2.0 mmol), and potassium carbonate (276 mg, 2.0 mmol) in DMF (5 mL) was stirred at room temperature for 5 h. Water (20 mL) was added, and the formed solid was filtered, washed with water, and solid dried to give **10** as an off-white solid (390 mg, 66%); mp 239–240 °C. 1H NMR (500 MHz, $CDCl_3$) δ 7.76 (d, J = 8.2 Hz, 1H), 7.74–7.69 (m, 1H), 7.60 (d, J = 8.2 Hz, 1H), 7.41 (t, J = 7.4 Hz, 1H), 7.30–7.26 (m, 2H), 7.24–7.19 (m, 2H), 6.08 (d, J = 6.7 Hz, 1H), 5.27–5.15 (m, 1H), 3.53 (dd, J = 16.2, 7.0 Hz, 2H), 3.00 (dd, J = 16.2, 4.0 Hz, 2H). ^{13}C NMR (125 MHz, $CDCl_3$) δ 160.6, 157.8, 151.0, 140.7, 133.6, 128.0, 127.1, 126.2, 125.1, 120.8, 113.3, 52.6, 40.2. MS (ESI) m/z $[M + H]^+$: calcd, 296.09; found, 296.13.

General Procedure for 11a–11h. A mixture of 2-chloro-N-(2,3-dihydro-1H-inden-2-yl)quinazolin-4-amine **10** (148 mg, 0.5 mmol), boronic acid (0.5 mmol), $Pd(PPh_3)_4$ (58 mg, 0.05 mmol), potassium carbonate (276 mg, 2.0 mmol) in dioxane (10 mL), and water (1.5 mL) was heated at 85 °C under an argon atmosphere for 16 h. Water (5 mL) was added, and the mixture was extracted with EtOAc (25 mL \times 3). The combined organic phase was washed with brine (15 mL), dried (Na_2SO_4), filtered, evaporated, and purified by flash chromatography to give product.

Analytical Data for Compounds 11a–11h. N-(2,3-Dihydro-1H-inden-2-yl)-2-(4-methylpyridin-3-yl)quinazolin-4-amine (11a). White solid (125 mg, 71%); mp 170–172 °C. 1H NMR (500 MHz, $CDCl_3$) δ 9.16 (s, 1H), 8.50 (d, J = 5.0 Hz, 1H), 7.91 (d, J = 7.9 Hz, 1H), 7.75 (ddd, J = 8.3, 7.0, 1.2 Hz, 1H), 7.67 (d, J = 7.8 Hz, 1H), 7.49–7.42 (m, 1H), 7.29 (dd, J = 5.3, 3.4 Hz, 2H), 7.25–7.19 (m, 3H), 5.94 (d, J = 7.0 Hz, 1H), 5.26 (tdd, J = 7.1, 4.4, 2.6 Hz, 1H), 3.54 (dd, J = 16.2, 7.1 Hz, 2H), 3.04 (dd, J = 16.2, 4.4 Hz, 2H), 2.72 (s, 3H). ^{13}C NMR (125 MHz, $CDCl_3$) δ 161.1, 159.1, 151.3, 150.1, 149.2, 146.6, 140.9, 135.4, 132.7, 128.8, 126.8, 125.9, 124.9, 120.7, 113.2, 52.3, 40.2, 21.0. HRMS (ESI): calcd for $C_{23}H_{21}N_4$ $[M + H]^+$, 353.1761; found, 353.1765.

N-(2,3-Dihydro-1H-inden-2-yl)-2-(5-methylpyridin-3-yl)-quinazolin-4-amine (11b). Yellow solid (134 mg, 76%); mp 200–201 °C. 1H NMR (500 MHz, $CDCl_3$) δ 9.59 (d, J = 1.6 Hz, 1H), 8.63 (s, 1H), 8.53 (d, J = 1.6 Hz, 1H), 7.92 (d, J = 8.0 Hz, 1H), 7.77–7.71 (m, 1H), 7.66 (d, J = 7.8 Hz, 1H), 7.45–7.38 (m, 1H), 7.30 (dd, J = 5.3, 3.4 Hz, 2H), 7.23 (dd, J = 5.5, 3.2 Hz, 2H), 5.95 (d, J = 6.8 Hz, 1H), 5.40–5.29 (m, 1H), 3.61 (dd, J = 16.2, 7.2 Hz, 2H), 3.08 (dd, J = 16.2, 4.8 Hz, 2H), 2.45 (s, 3H). ^{13}C NMR (125 MHz, $CDCl_3$) δ 159.3, 158.8, 151.2, 150.3, 147.6, 141.1, 136.0, 134.0, 132.7, 132.6, 128.7, 126.8, 125.7, 124.9, 120.8, 113.9, 52.4, 40.1, 18.5. HRMS (ESI): calcd for $C_{23}H_{21}N_4$ $[M + H]^+$, 353.1761; found, 353.1757.

N-(2,3-Dihydro-1H-inden-2-yl)-2-(6-methylpyridin-3-yl)-quinazolin-4-amine (11c). Yellow solid (129 mg, 73%); mp 175–176 °C. 1H NMR (500 MHz, $CDCl_3$) δ 9.66 (d, J = 1.9 Hz, 1H), 8.69 (dd, J = 8.1, 2.2 Hz, 1H), 7.89 (d, J = 8.0 Hz, 1H), 7.73–7.68 (m, 1H), 7.63 (d, J = 7.9 Hz, 1H), 7.41–7.36 (m, 1H), 7.29–7.25 (m, 2H), 7.23–7.19 (m, 3H), 5.91 (d, J = 6.6 Hz, 1H), 5.33–5.23 (m, 1H), 3.58 (dd, J = 16.2, 7.2 Hz, 2H), 3.06 (dd, J = 16.1, 4.8 Hz, 2H), 2.62 (s, 3H). ^{13}C NMR (125 MHz, $CDCl_3$) δ 159.8, 159.2, 158.8, 150.4, 149.7, 141.0, 136.0, 132.6, 131.6, 128.8, 126.9, 125.6, 124.9, 122.7, 120.5, 113.7, 52.5, 40.2, 24.5. HRMS (ESI): calcd for $C_{23}H_{21}N_4$ $[M + H]^+$, 353.1761; found, 353.1767.

N-(2,3-Dihydro-1H-inden-2-yl)-2-phenylquinazolin-4-amine (11d). White solid (84 mg, 50%); mp 221–223 °C. 1H NMR (500 MHz, $CDCl_3$) δ 8.64–8.56 (m, 2H), 7.93 (d, J = 8.3 Hz, 1H), 7.72 (ddd, J = 8.3, 7.0, 1.3 Hz, 1H), 7.64 (d, J = 7.8 Hz, 1H), 7.53–7.46 (m, 3H), 7.39 (ddd, J = 8.1, 7.0, 1.1 Hz, 1H), 7.31 (dd, J = 5.3, 3.3 Hz, 2H), 7.24 (dd, J = 5.5, 3.2 Hz, 2H), 5.86 (d, J = 6.6 Hz, 1H), 5.38 (tdd, J = 7.1, 5.1, 2.1 Hz, 1H), 3.61 (dd, J = 16.1, 7.2 Hz, 2H), 3.08 (dd, J = 16.1, 5.0 Hz, 2H). ^{13}C NMR (125 MHz, $CDCl_3$) δ 160.4, 159.2, 150.5, 141.1, 138.9, 132.5, 130.1, 128.9, 128.4, 128.2, 126.8, 125.3, 125.0,

120.4, 113.6, 52.4, 40.2. HRMS (ESI): calcd for $C_{23}H_{20}N_3$ $[M + H]^+$, 338.1652; found, 338.1647.

N-(2,3-Dihydro-1H-inden-2-yl)-2-(pyridin-4-yl)quinazolin-4-amine (11e). Brown solid (59 mg, 35%); mp 246–247 °C. 1H NMR (500 MHz, $CDCl_3$) δ 8.74 (d, J = 5.5 Hz, 2H), 8.40 (d, J = 5.9 Hz, 2H), 7.93 (d, J = 8.2 Hz, 1H), 7.78–7.70 (m, 1H), 7.67 (d, J = 8.1 Hz, 1H), 7.48–7.39 (m, 1H), 7.29 (dd, J = 5.2, 3.4 Hz, 2H), 7.22 (dd, J = 5.4, 3.3 Hz, 2H), 5.99 (d, J = 6.7 Hz, 1H), 5.37–5.29 (m, 1H), 3.59 (dd, J = 16.2, 7.2 Hz, 2H), 3.07 (dd, J = 16.1, 4.8 Hz, 2H). ^{13}C NMR (125 MHz, $CDCl_3$) δ 159.4, 158.4, 150.2, 150.2, 146.4, 141.0, 132.8, 129.2, 126.9, 126.3, 125.0, 122.3, 120.6, 114.1, 77.2, 77.0, 76.7, 52.5, 40.1. HRMS (ESI): calcd for $C_{22}H_{19}N_4$ $[M + H]^+$, 339.1604; found, 339.1608.

N-(2,3-Dihydro-1H-inden-2-yl)-2-(thiophen-2-yl)quinazolin-4-amine (11f). Off-white solid (68 mg, 40%); mp 243–246 °C. 1H NMR (500 MHz, $CDCl_3$) δ 8.08 (d, J = 3.1 Hz, 1H), 7.85 (d, J = 8.4 Hz, 1H), 7.69 (t, J = 7.6 Hz, 1H), 7.61 (d, J = 8.1 Hz, 1H), 7.45 (d, J = 4.9 Hz, 1H), 7.38–7.33 (m, 1H), 7.32–7.27 (m, 2H), 7.23 (dd, J = 5.3, 3.3 Hz, 2H), 7.18–7.13 (m, 1H), 5.88 (d, J = 6.3 Hz, 1H), 5.31–5.24 (m, 1H), 3.60 (dd, J = 16.2, 7.2 Hz, 2H), 3.06 (dd, J = 16.2, 5.0 Hz, 2H). ^{13}C NMR (125 MHz, $CDCl_3$) δ 159.0, 157.3, 150.4, 145.2, 141.1, 132.6, 129.0, 128.5, 128.2, 127.9, 126.8, 125.1, 124.9, 120.5, 113.5, 52.5, 40.1. HRMS (ESI): calcd for $C_{21}H_{18}N_3S$ $[M + H]^+$, 344.1216; found, 344.1218.

N-(2,3-Dihydro-1H-inden-2-yl)-2-(thiophen-3-yl)quinazolin-4-amine (11g). Yellow solid (75 mg, 44%); mp 232–233 °C. 1H NMR (500 MHz, $CDCl_3$) δ 8.34 (d, J = 3.0 Hz, 1H), 8.02 (dd, J = 5.0, 0.9 Hz, 1H), 7.87 (d, J = 8.3 Hz, 1H), 7.74–7.65 (m, 1H), 7.62 (d, J = 8.0 Hz, 1H), 7.42–7.34 (m, 2H), 7.30 (dd, J = 5.2, 3.4 Hz, 2H), 7.25–7.21 (m, 2H), 5.85 (d, J = 6.5 Hz, 1H), 5.36–5.25 (m, 1H), 3.58 (dd, J = 16.2, 7.2 Hz, 2H), 3.07 (dd, J = 16.1, 5.0 Hz, 2H). ^{13}C NMR (125 MHz, $CDCl_3$) δ 159.1, 157.8, 150.5, 143.1, 141.1, 132.5, 128.6, 127.9, 127.4, 126.8, 125.4, 125.1, 124.9, 120.5, 113.5, 52.3, 40.2. HRMS (ESI): calcd for $C_{21}H_{18}N_3S$ $[M + H]^+$, 344.1216; found, 344.1215.

N-(2,3-Dihydro-1H-inden-2-yl)-2-(furan-2-yl)quinazolin-4-amine (11h). Pale-yellow solid (80 mg, 49%); mp 231–232 °C. 1H NMR (500 MHz, $CDCl_3$) δ 7.96 (d, J = 8.4 Hz, 1H), 7.73–7.67 (m, 1H), 7.67–7.61 (m, 2H), 7.41–7.32 (m, 2H), 7.32–7.26 (m, 2H), 7.25–7.21 (m, 2H), 6.57 (dd, J = 3.3, 1.7 Hz, 1H), 5.98 (d, J = 6.8 Hz, 1H), 5.34–5.20 (m, 1H), 3.57 (dd, J = 16.1, 7.2 Hz, 2H), 3.05 (dd, J = 16.1, 5.0 Hz, 2H). ^{13}C NMR (125 MHz, $CDCl_3$) δ 159.1, 153.7, 153.4, 150.1, 144.6, 141.0, 132.7, 128.8, 126.8, 125.3, 124.9, 120.5, 113.7, 113.1, 111.8, 52.3, 40.1. HRMS (ESI): calcd for $C_{21}H_{18}N_3O$ $[M + H]^+$, 328.1444; found, 328.1448.

Enzymatic Assays. 4-Methylumbelliferyl β -D-glucopyranoside (4MU- β -Glc), 4-methylumbelliferyl α -D-glucopyranoside, 4-methylumbelliferyl α -D-galactopyranoside, and buffer components were purchased from Sigma-Aldrich (St. Louis, MO). The recombinant wild-type GCase enzyme velaglycerase alfa (Vpriv, Shire Human Genetic Therapies, Inc.), acid α -glucosidase enzyme alglucosidase alfa (Lumizyme, Genzyme Corporation), α -galactosidase A enzyme agalsidase beta (Fabrazyme, Genzyme Corporation) were used in activity assays. The GCase activity assay buffer was composed of 50 mM citric acid, 176 mM K_2HPO_4 , and 0.01% Tween-20 at pH 5.0, pH 5.9 and pH 7.0. A solution of 1 M sodium hydroxide and 1 M glycine (pH 10) was used as the stop solution for all three enzyme activity assays.

GCase Enzyme Activity Assay. The compounds in DMSO solution (0.5 μ L/well) were transferred to a black 96-well plate (the final titration started from 100 μ M, a 12- or 24-point 2-fold dilution series). Enzyme solution (33.5 μ L, 7.5 nM final concentration, in pH 5.9 buffer) was transferred to the wells. After 5 min of incubation at room temperature, the enzyme reaction was initiated by the addition of blue substrate (4MU- β -Glc) (33 μ L/well). The final concentration of the blue substrate was 1.5 mM. The blue substrate reaction was terminated by the addition of 33 μ L/well stop solution (1 M NaOH and 1 M glycine mixture, pH 10) after 30 min of incubation at 37 °C. The fluorescence was then measured in a Biotek Synergy H1 multimode plate reader with Ex = 365 nm and Em = 440 nm. The

selected compounds were further assayed under pH 5.0 and pH 7.0 to evaluate their selectivity under various pH conditions.

Enzyme Kinetic Assay.²⁰ The substrate resorufin β -D-glucopyranoside was diluted to five concentrations, ranging from 30 to 150 μ M. Seven concentrations of inhibitors (between 0.5- and 5-fold of IC_{50} value) and a DMSO control were added to the enzyme solution. The final enzyme concentration was 10 nM to give a linear reaction over 10 min. Enzyme kinetics were measured by the addition of 66 μ L of substrate to a 96-well assay plate, followed by 33 μ L of enzyme solution (with or without inhibitor) using a dispense module on a Biotek Synergy H1 multimode plate reader. The increase in product fluorescence was measured at 1 min intervals for 10 min in the plate reader. The rate of product formation was calculated by converting the fluorescence units to nanomoles of product per minute using a standard curve of the free fluorophore, resorufin.

Enzyme Selectivity Assays. The acid α -glucosidase and α -galactosidase A enzyme activity assay methods were similar to the GCase enzyme activity assay above with slight modifications. The buffer for the two enzyme assays consisted of 50 mM citric acid, 176 mM K_2HPO_4 , and 0.01% Tween-20 at pH 4.8. The final enzyme concentrations for acid α -glucosidase and α -galactosidase A were 8 and 1 nM, respectively. The substrate concentrations for these related enzymes were at 0.16 and 0.4 mM, respectively.

Fluorescence Thermal Shift Analysis.³² A robotic pipeline in the High Throughput Analysis Laboratory (HTAL) was used for protein–ligand screening by fluorescence thermal shift (FTS) analysis. The pipeline used a Mosquito robot (TTP Labtech) for protein dispensing and an Echo 550 (Labcyte) to add compounds. Thermal scanning coupled with fluorescence detection was performed on a real-time PCR machine CFX384 (Bio-Rad Laboratories). The assay was run in 384-well PCR plates, using 10 μ L citric acid/ K_2HPO_4 buffer (50 mM citric acid, 150 mM K_2HPO_4 , pH 5.0) per well. The assay concentration for protein was 1 μ M and that for Sypro Orange (Invitrogen) was 5 \times . Protein was premixed with Sypro Orange and dispensed to a plate first, and compounds were added. Final concentrations of compounds ranged from 0.5 to 200 μ M. Then the plate was sealed with an optical seal, shaken, and centrifuged. The thermal scan was from 10 to 95 $^{\circ}$ C with a temperature ramp rate of 1.5 $^{\circ}$ C/min. The fluorescence was recorded every 10 s. Data analysis and report generation were performed using the in-house software excelFTS. The T_m of wild-type GCase was found to follow a logarithmic dose-dependent trend when denaturation was performed in the presence of isofagomine or selected compounds.

N370S Cell Culture and Compound Treatment. The N370S fibroblast cell line was obtained from Coriell, GM00372, cultured in DMEM medium (Life Tech) including 1% v/v L-glutamine 200 mM (Life Tech), 1% v/v pen strep (Life Tech), 10% FBS (Life Tech) at 37 $^{\circ}$ C, and 5% CO_2 and treated with different compounds at indicated concentrations. The same volume of DMSO (0.1% v/v) was used as a control. After a 3-day treatment, cells were washed with inhibitor free media three times and followed by 1% Triton X-100 lysis buffer to lyse cells. Protein concentrations were measured with a Bicinchoninic Acid Kit (Sigma), and the GCase activity was determined at pH 5.5.

Deglycosylation of Proteins/Molecular Shift Assay.³³ To study the ER and post-ER localization of the N370S GCase mutant after incubation with increasing concentrations of **11g**, EndoH and PNGaseF digestions were performed. For both reactions, 10–20 μ g of protein was used and the experimental procedure was performed according to the manufacturer's handbook (New England Biolabs). A positive digestion resulted in a shift in molecular size after the protein was subjected to SDS/PAGE.

Western Blot. Proteins were denatured in 20% SDS sample buffer at 100 $^{\circ}$ C for 10 min, 4–20% Tris-Glycine gel (Life Tech) was used for gels, and Trans-Blot Turbo Nitrocellulose kit (Bio-Rad) was used for membrane transfer. GCase antibody (Sigma-Aldrich) and GAPDH primary antibodies (EMD Millipore) were incubated with the membranes overnight, then the incubated membranes were treated with the secondary antibody (Peroxidase-AffiniPure Goat Anti-Rabbit/Mouse IgG (H+L), Jackson ImmunoResearch Lab) for 30 min.

Chemidoc MP system (Bio-Rad) was used to scan the membranes and analyze the imaging.

■ ASSOCIATED CONTENT

§ Supporting Information

The Supporting Information is available free of charge on the ACS Publications website at DOI: 10.1021/acs.jmedchem.6b00930.

¹H and ¹³C NMR spectra of **4**, **6c**, **7a**, **7b**, **8c**, **9a**, **9b**, **9c**, **11b**, **11d**, **11f**, **11g**, and **11h** (PDF)
Molecular formula strings (CSV)

■ AUTHOR INFORMATION

Corresponding Authors

*For R.B.S.: phone, 847-491-5653; Fax, 847-491-7713; E-mail, Agman@chem.northwestern.edu.

*For D.K.: phone, 312-503-3936; fax, 312-503-3950; E-mail, krainc@northwestern.edu.

Notes

The authors declare no competing financial interest.

■ ACKNOWLEDGMENTS

This work was supported by R01NS076054 (to D.K.). J.Z. and M.S. are also supported by the fellowships from Lysosomal Therapeutics Inc. (Cambridge, MA) and the Deutsche Forschungsgemeinschaft (Heisenberg Programme), respectively. This work made use of the IMSERC at Northwestern University, which has received support from the Soft and Hybrid Nanotechnology Experimental (SHyNE) Resource (NSF NNCI-1542205), the State of Illinois, and the International Institute for Nanotechnology (IIN). We thank H. Goudarzi and S. Shafaie in IMSERC at Northwestern University for their assistance with HRMS experiments and C. H. Luan in Northwestern University's High Throughput Analysis Laboratory for his assistance with thermal denaturation experiments.

■ ABBREVIATIONS USED

GD, Gaucher's disease; GCase, β -glucocerebrosidase; ER, endoplasmic reticulum; ERT, enzyme replacement therapy; SRT, substrate reduction therapy; PC, pharmacological chaperone; IFG, isofagomine; PD, Parkinson's disease; DLB, dementia with Lewy bodies; SAR, structure–activity relationship; GAA, acid α -glucosidase; GLA, α -galactosidase A

■ REFERENCES

- (1) Grabowski, G. A. Phenotype, diagnosis, and treatment of Gaucher's disease. *Lancet* **2008**, 372, 1263–1271.
- (2) Bennett, L. L.; Mohan, D. Gaucher disease and its treatment options. *Ann. Pharmacother.* **2013**, 47, 1182–1193.
- (3) Grabowski, G. A.; Zimran, A.; Ida, H. Gaucher disease types 1 and 3: Phenotypic characterization of large populations from the ICGG Gaucher Registry. *Am. J. Hematol.* **2015**, 90 (Suppl S1), S12–S18.
- (4) Hruska, K. S.; LaMarca, M. E.; Scott, C. R.; Sidransky, E. Gaucher disease: mutation and polymorphism spectrum in the glucocerebrosidase gene (GBA). *Hum. Mutat.* **2008**, 29, 567–583.
- (5) Sawkar, A. R.; Cheng, W. C.; Beutler, E.; Wong, C. H.; Balch, W. E.; Kelly, J. W. Chemical chaperones increase the cellular activity of N370S beta -glucosidase: a therapeutic strategy for Gaucher disease. *Proc. Natl. Acad. Sci. U. S. A.* **2002**, 99, 15428–15433.
- (6) Tekoah, Y.; Tzaban, S.; Kizhner, T.; Hainrichson, M.; Gantman, A.; Golemb, M.; Aviezer, D.; Shaaltiel, Y. Glycosylation and

functionality of recombinant beta-glucocerebrosidase from various production systems. *Biosci. Rep.* **2013**, *33*, e00071.

(7) Aharon-Peretz, J.; Rosenbaum, H.; Gershoni-Baruch, R. Mutations in the glucocerebrosidase gene and Parkinson's disease in Ashkenazi Jews. *N. Engl. J. Med.* **2004**, *351*, 1972–1977.

(8) Sidransky, E.; Nalls, M. A.; Aasly, J. O.; Aharon-Peretz, J.; Annesi, G.; Barbosa, E. R.; Bar-Shira, A.; Berg, D.; Bras, J.; Brice, A.; Chen, C. M.; Clark, L. N.; Condroyer, C.; De Marco, E. V.; Durr, A.; Eblan, M. J.; Fahn, S.; Farrer, M. J.; Fung, H. C.; Gan-Or, Z.; Gasser, T.; Gershoni-Baruch, R.; Giladi, N.; Griffith, A.; Gurevich, T.; Januario, C.; Kropp, P.; Lang, A. E.; Lee-Chen, G. J.; Lesage, S.; Marder, K.; Mata, I. F.; Mirelman, A.; Mitsui, J.; Mizuta, I.; Nicoletti, G.; Oliveira, C.; Ottman, R.; Orr-Urtreger, A.; Pereira, L. V.; Quattrone, A.; Rogaeva, E.; Rolfs, A.; Rosenbaum, H.; Rozenberg, R.; Samii, A.; Samadpour, T.; Schulte, C.; Sharma, M.; Singleton, A.; Spitz, M.; Tan, E. K.; Tayebi, N.; Toda, T.; Troiano, A. R.; Tsuji, S.; Wittstock, M.; Wolfsberg, T. G.; Wu, Y. R.; Zabetian, C. P.; Zhao, Y.; Ziegler, S. G. Multicenter analysis of glucocerebrosidase mutations in Parkinson's disease. *N. Engl. J. Med.* **2009**, *361*, 1651–1661.

(9) Schapira, A. H. V.; Olanow, C. W.; Greenamyre, J. T.; Bezd, E. Slowing of neurodegeneration in Parkinson's disease and Huntington's disease: future therapeutic perspectives. *Lancet* **2014**, *384*, 545–555.

(10) Sidransky, E.; Lopez, G. The link between the GBA gene and parkinsonism. *Lancet Neurol.* **2012**, *11*, 986–998.

(11) Lin, M. K.; Farrer, M. J. Genetics and genomics of Parkinson's disease. *Genome Med.* **2014**, *6*, 48.

(12) Mazzulli, J. R.; Xu, Y. H.; Sun, Y.; Knight, A. L.; McLean, P. J.; Caldwell, G. A.; Sidransky, E.; Grabowski, G. A.; Krainc, D. Gaucher disease glucocerebrosidase and alpha-synuclein form a bidirectional pathogenic loop in synucleinopathies. *Cell* **2011**, *146*, 37–52.

(13) Sardi, S. P.; Clarke, J.; Viel, C.; Chan, M.; Tamsett, T. J.; Treleaven, C. M.; Bu, J.; Sweet, L.; Passini, M. A.; Dodge, J. C.; Yu, W. H.; Sidman, R. L.; Cheng, S. H.; Shihabuddin, L. S. Augmenting CNS glucocerebrosidase activity as a therapeutic strategy for parkinsonism and other Gaucher-related synucleinopathies. *Proc. Natl. Acad. Sci. U. S. A.* **2013**, *110*, 3537–3542.

(14) Sybertz, E.; Krainc, D. Development of targeted therapies for Parkinson's disease and related synucleinopathies. *J. Lipid Res.* **2014**, *55*, 1996–2003.

(15) Wang, G. N.; Reinkensmeier, G.; Zhang, S. W.; Zhou, J.; Zhang, L. R.; Zhang, L. H.; Butters, T. D.; Ye, X. S. Rational design and synthesis of highly potent pharmacological chaperones for treatment of N370S mutant Gaucher disease. *J. Med. Chem.* **2009**, *52*, 3146–3149.

(16) Trapero, A.; Gonzalez-Bulnes, P.; Butters, T. D.; Llebaria, A. Potent aminocyclitol glucocerebrosidase inhibitors are subnanomolar pharmacological chaperones for treating gaucher disease. *J. Med. Chem.* **2012**, *55*, 4479–4488.

(17) Sawkar, A. R.; Schmitz, M.; Zimmer, K. P.; Reczek, D.; Edmunds, T.; Balch, W. E.; Kelly, J. W. Chemical chaperones and permissive temperatures alter localization of Gaucher disease associated glucocerebrosidase variants. *ACS Chem. Biol.* **2006**, *1*, 235–251.

(18) Steet, R. A.; Chung, S.; Wustman, B.; Powe, A.; Do, H.; Kornfeld, S. A. The iminosugar isofagomine increases the activity of N370S mutant acid beta-glucosidase in Gaucher fibroblasts by several mechanisms. *Proc. Natl. Acad. Sci. U. S. A.* **2006**, *103*, 13813–13818.

(19) Butters, T. D.; Dwek, R. A.; Platt, F. M. Imino sugar inhibitors for treating the lysosomal glycosphingolipidoses. *Glycobiology* **2005**, *15*, 43R–52R.

(20) Zheng, W.; Padia, J.; Urban, D. J.; Jadhav, A.; Goker-Alpan, O.; Simeonov, A.; Goldin, E.; Auld, D.; LaMarca, M. E.; Ingles, J.; Austin, C. P.; Sidransky, E. Three classes of glucocerebrosidase inhibitors identified by quantitative high-throughput screening are chaperone leads for Gaucher disease. *Proc. Natl. Acad. Sci. U. S. A.* **2007**, *104*, 13192–13197.

(21) Marugan, J. J.; Zheng, W.; Motabar, O.; Southall, N.; Goldin, E.; Westbroek, W.; Stubblefield, B. K.; Sidransky, E.; Aungst, R. A.; Lea, W. A.; Simeonov, A.; Leister, W.; Austin, C. P. Evaluation of

quinazoline analogues as glucocerebrosidase inhibitors with chaperone activity. *J. Med. Chem.* **2011**, *54*, 1033–1058.

(22) Marugan, J. J.; Huang, W.; Motabar, O.; Zheng, W.; Xiao, J.; Patnaik, S.; Southall, N.; Westbroek, W.; Lea, W. A.; Simeonov, A.; Goldin, E.; Debernardi, M. A.; Sidransky, E. Non-iminosugar glucocerebrosidase small molecule chaperones. *MedChemComm* **2012**, *3*, 56–60.

(23) Tropak, M. B.; Kornhaber, G. J.; Rigat, B. A.; Maegawa, G. H.; Buttner, J. D.; Blanchard, J. E.; Murphy, C.; Tuske, S. J.; Coales, S. J.; Hamuro, Y.; Brown, E. D.; Mahuran, D. J. Identification of pharmacological chaperones for Gaucher disease and characterization of their effects on beta-glucocerebrosidase by hydrogen/deuterium exchange mass spectrometry. *ChemBioChem* **2008**, *9*, 2650–2662.

(24) Huang, W.; Zheng, W.; Urban, D. J.; Ingles, J.; Sidransky, E.; Austin, C. P.; Thomas, C. J. N4-phenyl modifications of N2-(2-hydroxy)ethyl-6-(pyrrolidin-1-yl)-1,3,5-triazine-2,4-diamines enhance glucocerebrosidase inhibition by small molecules with potential as chemical chaperones for Gaucher disease. *Bioorg. Med. Chem. Lett.* **2007**, *17*, 5783–5789.

(25) Storz, T.; Heid, R.; Zeldis, J.; Hoagland, S. M.; Rapisardi, V.; Hollywood, S.; Morton, G. Convenient and practical one-pot synthesis of 4-chloropyrimidines via a novel chloroimidate annulation. *Org. Process Res. Dev.* **2011**, *15*, 918–924.

(26) Urban, D. J.; Zheng, W.; Goker-Alpan, O.; Jadhav, A.; Lamarca, M. E.; Ingles, J.; Sidransky, E.; Austin, C. P. Optimization and validation of two miniaturized glucocerebrosidase enzyme assays for high throughput screening. *Comb. Chem. High Throughput Screening* **2008**, *11*, 817–824.

(27) Aguilar-Moncalvo, M.; Garcia-Moreno, M. I.; Trapero, A.; Egidio-Gabas, M.; Llebaria, A.; Garcia Fernandez, J. M.; Ortiz Mellet, C. O. Bicyclic (galacto)nojirimycin analogues as glycosidase inhibitors: Effect of structural modifications in their pharmacological chaperone potential towards beta-glucocerebrosidase. *Org. Biomol. Chem.* **2011**, *9*, 3698–3713.

(28) Trapero, A.; Alfonso, I.; Butters, T. D.; Llebaria, A. Polyhydroxylated bicyclic isoureas and guanidines are potent glucocerebrosidase inhibitors and nanomolar enzyme activity enhancers in Gaucher cells. *J. Am. Chem. Soc.* **2011**, *133*, 5474–5484.

(29) Berger, Z.; Perkins, S.; Ambroise, C.; Oborski, C.; Calabrese, M.; Noell, S.; Riddell, D.; Hirst, W. D. Tool compounds robustly increase turnover of an artificial substrate by glucocerebrosidase in human brain lysates. *PLoS One* **2015**, *10*, e0119141.

(30) Lo, M. C.; Aulabaugh, A.; Jin, G.; Cowling, R.; Bard, J.; Malamas, M.; Ellestad, G. Evaluation of fluorescence-based thermal shift assays for hit identification in drug discovery. *Anal. Biochem.* **2004**, *332*, 153–159.

(31) Matulis, D.; Kranz, J. K.; Salemme, F. R.; Todd, M. J. Thermodynamic stability of carbonic anhydrase: measurements of binding affinity and stoichiometry using ThermoFluor. *Biochemistry* **2005**, *44*, 5258–5266.

(32) Filippova, E. V.; Luan, C. H.; Dunne, S. F.; Kiryukhina, O.; Minasov, G.; Shuvalova, L.; Anderson, W. F. Structural characterization of a hypothetical protein: a potential agent involved in trimethylamine metabolism in *Catenulispora acidiphila*. *J. Struct. Funct. Genomics* **2014**, *15*, 33–40.

(33) Zunke, F.; Andresen, L.; Wesseler, S.; Groth, J.; Arnold, P.; Rothaug, M.; Mazzulli, J. R.; Krainc, D.; Blanz, J.; Saftig, P.; Schwake, M. Characterization of the complex formed by beta-glucocerebrosidase and the lysosomal integral membrane protein type-2. *Proc. Natl. Acad. Sci. U. S. A.* **2016**, *113*, 3791–3796.